N89-18390

S12-74
175241
35P

CRYOGENIC MIRROR ANALYSIS

S. Nagy

1. INTRODUCTION

Due to extraordinary distances scanned by modern telescopes, optical surfaces in such telescopes must be manufactured to unimaginable standards of perfection of a few thousandths of a centimeter. Upon what seems a perfectly ground and polished mirror, there will lie ripples, bumps, valleys, and a variety of aberrations and distortions. To detect these imperfections requires an intricately tuned optical system in conjunction with a phase-shift interferometer. The goal of the Astrophysical Experiments Branch group at NASA Ames was to be able to detect imperfections of less than 1/20 of a wavelength of light, for application in the building of the mirror for the Space Infrared Telescope Facility (SIRTF). Because the mirror must be kept very cold while in space, another factor comes into effect: cryogenics.

Cryogenics refers to very cold liquids or surfaces, such as liquid helium (4.2 Kelvin). Since the mirror that will be used in SIRTF must detect radiation in the infrared range, any stray radiation from the telescope facility would degrade the quality of the image received from outer space. For this reason, the mirror must be cleverly surrounded by various heat shields of liquid helium, liquid nitrogen, and reflective coatings. But like any other surface that is cooled, the mirror will bend and twist out of its normal shape. This results in erroneous images.

How does the mirror become distorted? Is there any way to correct its aberrations, so as to recieve a clear image? How does the light energy reflect from a warped mirror? These are some of the questions that are being answered by Cryogenic Mirror Testing/Analysis. This paper describes the process to test a specific mirror under cryogenic conditions; including the follow-up analysis accomplished through computer work. To better illustrate the process and analysis, we will follow a Pyrex Hex-Core mirror (Photo 5) through the process (referring to it as Mirror 1A) from the laser interferometry in the lab, to computer analysis via a computer program called FRINGE.

FRINGE has been an integral part of the Cryogenic Mirror Analysis giving Ames Research Center a fairly advanced computational tool for the analysis of an interferogram (an image describing the characteristics of an optical surface), which is vital to SIRTF. FRINGE has served as a solution to the problem of quantifying test data so that surface profile and other optical characteristics can be quantitatively determined.

> The program can be viewed as a collection of subroutines that the user can arrange to quantify a variety of test data and reduce it such that a high quality optical path difference (OPD) map is produced. With this map, other analysis subroutines can be used to test optic errors, perform image quality analyses, calculate aberration coefficients, determine residual errors, etc. *(Taken from FRINGE manual, Arizona Optical Sciences Center)*

2. MECHANICS OF THE ANALYSIS PROCESS

During this discussion of the lab set-up and procedure, refer to the diagrams and pictures in Appendix A and Appendix C, respectively. For analysis of how the mirror will perform under extreme cold conditions, it is first mounted to the bottom of the top section of the dewar assembly as seen in Photo 4. The mirror must be firmly and precisely mounted to avoid wobbling. The dewar assembly, as seen in Photo 3, is the apparatus by which the mirror can be cooled to nearly 4 Kelvin (liquid helium temperature) to simulate its environment in space. Diagram 1 is a section view of the entire dewar assembly as seen in Photo 3.

Once the test mirror has been attached, the bottom two components of the dewar are attached, and the cooling down process begins. The liquid helium and the liquid nitrogen tanks at the top of the dewar are filled, after the air is pumped out from between the walls of the dewar. The laser interferometer, Photo 2 and Diagram 2, has been turned on at this point and during the cooling of the mirror, the laser is manually kept the correct distance from the mirror to remain in focus, by use of a micrometer mount (on Diagram 2).

Carbon resistors placed on the mirror surface and the walls of the dewar, indicate the temperature. As the temperature approaches that of liquid helium (4.2 Kelvin), the interferometer is precisely focused so that a clear image exists. The path of the laser beam is as follows. (Refer to Diagram 2.) First the laser beam, generated by a Helium-Neon Laser, passes through an aperture to filter out any scatter radiation or fuzziness. Then the beam passes through a microscope objective, which concentrates and narrows the beam, toward a beam-splitter cube where the majority of the light is reflected upward toward the test mirror through a window opening in the bottom of the dewar assembly.

Let us imagine that the light travels upward toward the mirror in small packages. Upon reaching the mirror, the light is reflected. Note that the light, however, may not be returning along the same path as when it was traveling toward the mirror, because the mirror may be warped from the cryogenic conditions. The reflected package of light meets with one of the packages of light that have been reflected downward by the beam-splitter cube. Ideally, the two packages should coincide, but because the reflected package of light is distorted, the two packages do not always mesh. In the areas where they do not mesh, they neutralize each other. This is called destructive interference, thus producing dark lines on the interferogram (Photo 1). These streaks are named fringes.

The light zones are where the two packages of light did not cancel each other. Once the fringe pattern is in focus, a photograph is taken. This is the point at which the fringe analysis via computer begins.

Photographs taken in the laboratory of the interference fringe pattern are digitized by an Apple IIe and HiPad digitizing tablet. The photo is placed on the tablet, where the fringe lines are manually entered into the computer, fringe by fringe until the image on the computer screen resembles the pattern on the photograph. At this point, the computer converts the digitized coordinates into three-digit x/y coordinates (inch measurements without the decimal point). A hard copy of these coordinates is then generated for manual data entry into the VAX mainframe computer via a Tektronix terminal.

The digitized x/y coordinates of the fringe pattern are entered into the VAX as a file, each line having the x/y coordinates for a certain fringe. Various options are open to the user, depending on the type of mirror being used and the type of output desired. The following commands initiate the setting of parameters that can affect the output from the FRINGE program:

a. WEDGE: specifies the frequency of fringes to be scanned

b. COBS n: n is the fraction of the mirror radius represented by the hole

c. STEP: defines the contour interval for the contour map (fraction of wavelengths)

d. WIDTH: defines the fraction of the contour interval in which the characters will be printed, ranging from 0 to 1 where 0 will print characters only when they are identical to the contour value; a width of 1 will print characters at every position and the map will be filled with print (see RESULTS AND WHAT THEY MEAN, Contour Map).

3. RESULTS AND WHAT THEY MEAN

Once the data have been entered and the parameters have been set, FRINGE is run. A typical hard copy of the results from the calculations is included in Appendix B. Some of the important pieces of information are:

a. STREHL RATIO: a measure of how close the mirror is to the ideal, with 1 being the ideal; defined as: given r = RMS Surface Error

b. RMS SURFACE ERROR: root of the means of the squares of the Zernike polynomial coefficients; defined as:

c. CONTOUR MAP: a top view of the mirror surface showing the peaks and valleys, much like a topographic map, using the letters A-N for decreasing mirror surface, and the letters P-Z for increasing mirror surface

d. ZERNIKE POLYNOMIAL COEFFICIENTS: the terms of an endless series (truncated to 36 terms for practical purposes) that represents the aberrations found on the mirror surface

In addition to alphanumeric output, we have the option to generate color graphic plots. They are RED, GSPOT, and 3D Plot of Aberrations, as found in Appendix D. All of these plots have been created from the Zernike polynomial coefficients calculated on Mirror 1A. Refer to the first set of plots (Group I) in Appendix D during the discussion of the three different types of plots. They represent general plots of all the contributions obtained from Mirror 1A.

The first plot, 1A, describes the physical topography of the mirror surface in an exaggerated fashion. It provides for a visual understanding as to how all the aberrations combine to distort the mirror surface. Subsequently, the aberrations that combine to create the mirror surface, can be broken down, isolated, and categorized as being one of the following: Radial (Spherical), 1θ (Coma), 2θ (Astigmatism), 3θ, 4θ, and 5θ. We will look at all the distortions of Mirror 1A, except 5θ because of its negligible contribution in this case.

Plot IB is referred to as GSPOT (Geometric Spot Diagram), which is the result of a Geometric Ray Analysis showing the intersection of approximately 640 rays with the image plane and as a radial energy distribution function.

The last type of plot, the Radial Energy Distribution plot (RED) depicts the energy concentration percentage at a given radius from the center of the mirror. This is the energy that is reflected back from the mirror. Notice on Plot IC the sudden decline of energy between 0.00 and 0.80. This is due to the COBS parameter which defines the mirror as having a central hole. Therefore, no energy is reflected in that region.

The Radial Contributions, Group II plots, reflect a wave-like distortion from the center out. Thus the name spherical. The distortion is symmetrical, as is evident from the 3D plot, and from the GSPOT diagram. Also note the slight dip in the rise of the Radial Energy Curve. This is also a result of the undulations present on the mirror surface. The Group III plots show the characteristics of Coma distortion, which is quite minimal in this instance as seen from Plot IIIA.

The 2θ and 3θ Contribution plots are similar in that they both characterize a "potato chip-like" aberration in which there are distinct, symmetrical highs and lows. Note that the 2θ has only two highs and two lows, whereas the 3θ has three highs and three lows. And lastly, the 4θ Contribution, Group IV, which lacks a very significant contribution.

4. THE FUTURE OF CRYOGENIC MIRROR ANALYSIS AT NASA AMES

Through Cryogenic Mirror Analysis, the SIRTF group at Ames has been able to study the way different mirrors distort under extreme cold conditions. Berylium, glass, and pyrex mirrors of different shapes and sizes have been tested. The next step, yet untested, is to try to reconfigure a mirror in an optical manufacturing environment so that it will be an undistorted mirror at cryogenic temperatures. This can be accomplished by polishing the mirror at room temperature using the data acquired from cryogenic testing. Where a peak existed at cryogenic temperature, a valley would be polished at room temperature. And vice versa. Then, theoretically, when the mirror is cooled it would distort from a bad mirror surface at room temperature, to a perfect surface at cryogenic temperature. This is what remains to be discovered through intensive testing.

In addition to the next steps in mirror reconfiguration, a few lab improvements are being sought. Plans for a larger dewar to accommodate larger mirrors are in sight as well as the purchase of a real-time, phase-shift laser interferometry system that would increase the present accuracy of 1/20 of a wavelength to 1/50 of a wavelength, as well as avoiding the manual data entry into the VAX. With these plans in mind, Cryogenic Mirror Analysis Technology at Ames Research Center will become an even more powerful tool.

APPENDIX A: DIAGRAMS

APPENDIX B: COMPUTER PRINTOUT

APPENDIX C: PHOTOS

APPENDIX D: PLOTS

APPENDIX E: PROCESS FLOWCHART

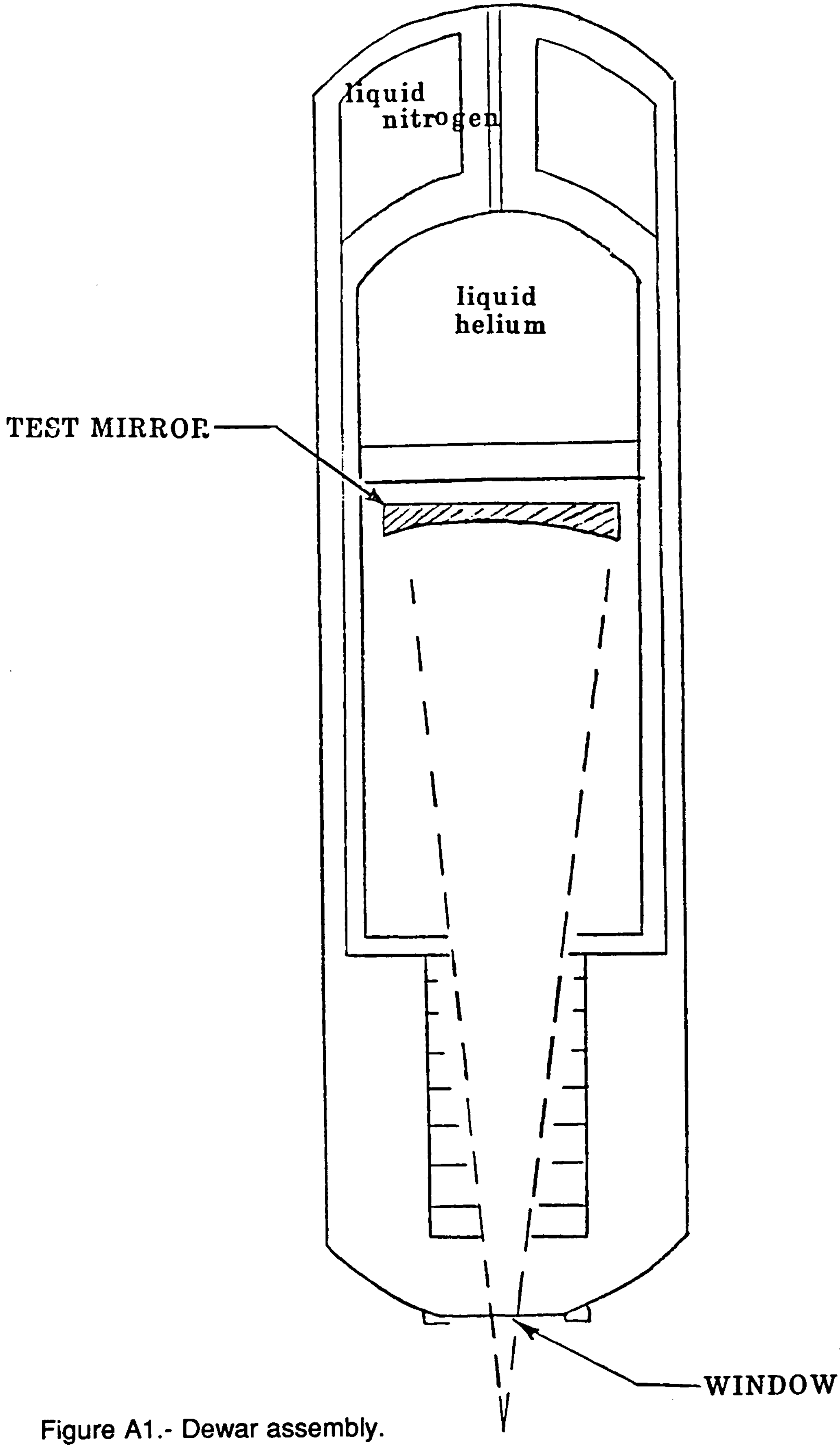

Figure A1.- Dewar assembly.

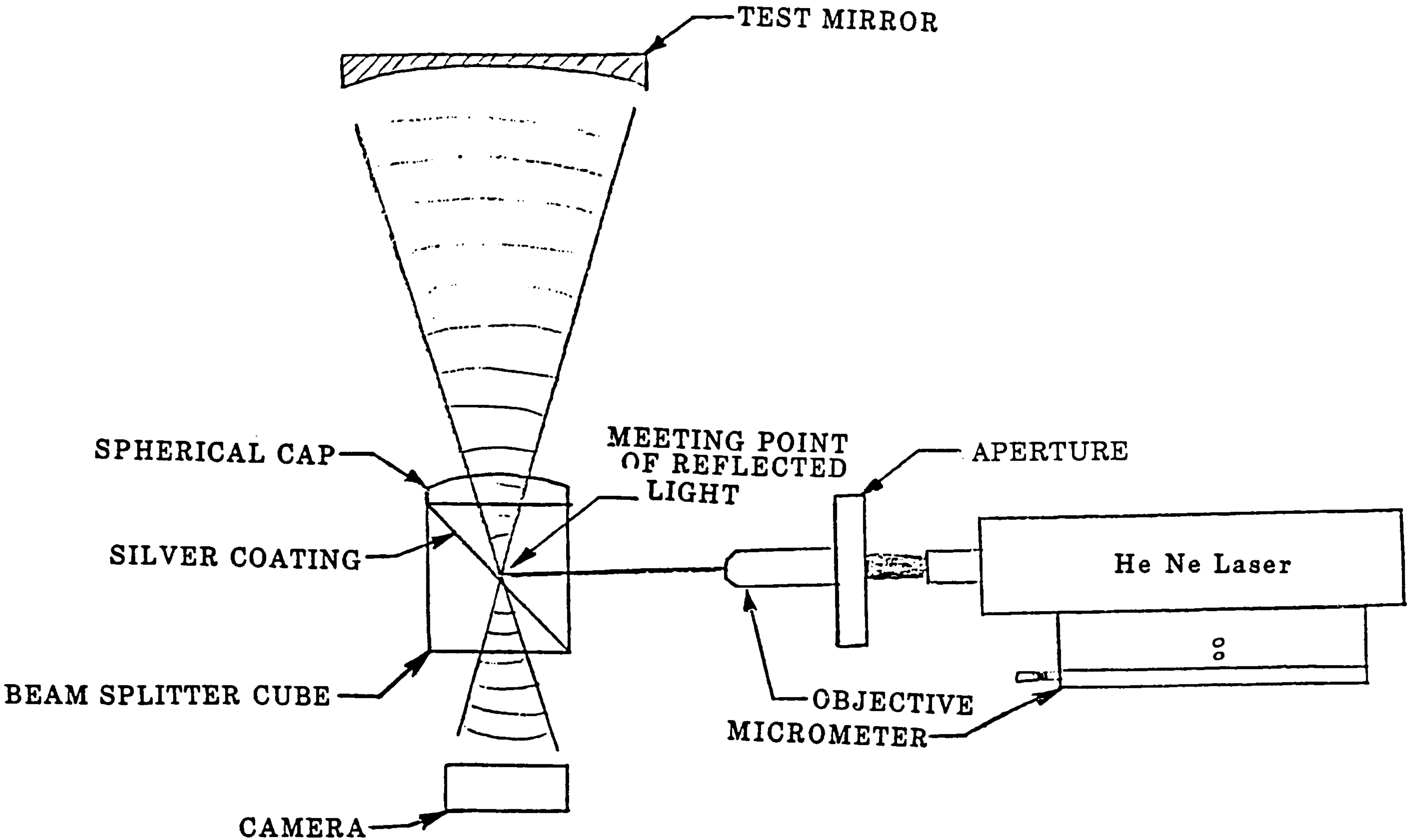

Figure A2.- Interferometer setup.

```
FRINGE ****** TECHNICAL PAPER-- SANDOR NAGY                       17-JUL-86 12:46:52
--FIDS 403 740  701 466  426 169  129 443
--LIST VERIFY
--TILT FOCUS
--WEDGE -.5
--COBS .25
--STEP .1
--WIDTH .8
--PART
--FSCAN
--END

APERTURE MASKING
TYPE        CAX         CAY         COX         COY
ELIP     1.0000      1.0000      0.2500      0.2500

--1      538 192   506 181   470 177   433 172   399 173   371 179   343 181   325 182
--       END
--2      562 209   523 205   480 204   435 206   391 208   350 209   313 212   276 223
--       248 232   214 248   END
--3      628 265   605 247   572 238   545 240   516 238   485 240   458 244   432 249
--       395 244   360 245   318 250   279 256   249 263   219 268   192 278   175 290
--       END
--4      650 294   613 282   528 274   488 276   443 274   368 280   289 289   202 305
--       153 335   END
--5      674 340   658 323   633 321   604 319   558 312   514 311   471 312   425 316
--       381 319   341 323   304 327   265 333   227 343   187 354   159 369   143 382
--       131 400   END
--6      681 383   647 373   548 357   503 352   462 354   410 358   363 363   307 367
--       267 371   236 378   197 395   171 403   146 416   128 437   END
--7      692 436   656 420   611 413   578 406   541 399   502 395   464 397   423 402
--       388 405   339 408   295 412   255 421   209 438   176 450   152 466   136 479
--       134 500   END
--8      695 476   614 459   574 448   540 442   489 442   436 443   405 446   383 450
--       365 455   344 354   297 456   270 465   240 479   211 486   181 499   156 513
--       146 533   141 552   END
--9      684 536   648 520   597 499   499 487   453 493   397 497   363 500   335 495
--         308 500   283 512   251 527   226 535   205 548   183 558   166 573   159 577
--       END
--10     668 576   579 557   508 533   467 537   427 540   375 540   346 545   308 554
--       278 564   243 580   214 589   191 592   179 605   END
--11     635 629   600 618   551 605   507 598   456 588   401 586   347 596   305 609
--       269 616   240 627   224 642   215 653   END
--12     577 686   568 668   510 651   472 646   437 645   403 649   368 650   314 660
--       281 666   269 677   267 686   265 697   END
--13     495 727   466 712   412 700   387 704   363 709   355 721   366 740   END
END OF DATA

PUPIL CENTER AND RADIUS
          XC             YC             RAD
     414.7500       454.5000       286.4809
```

Figure B1.- Computer printout 1.

ORIGINAL PAGE IS
OF POOR QUALITY

```
FRINGE ****** TECHNICAL PAPER-- SANDOR NAGY                    17-JUL-86 12:46:55
FRINGE VERIFICATION
```

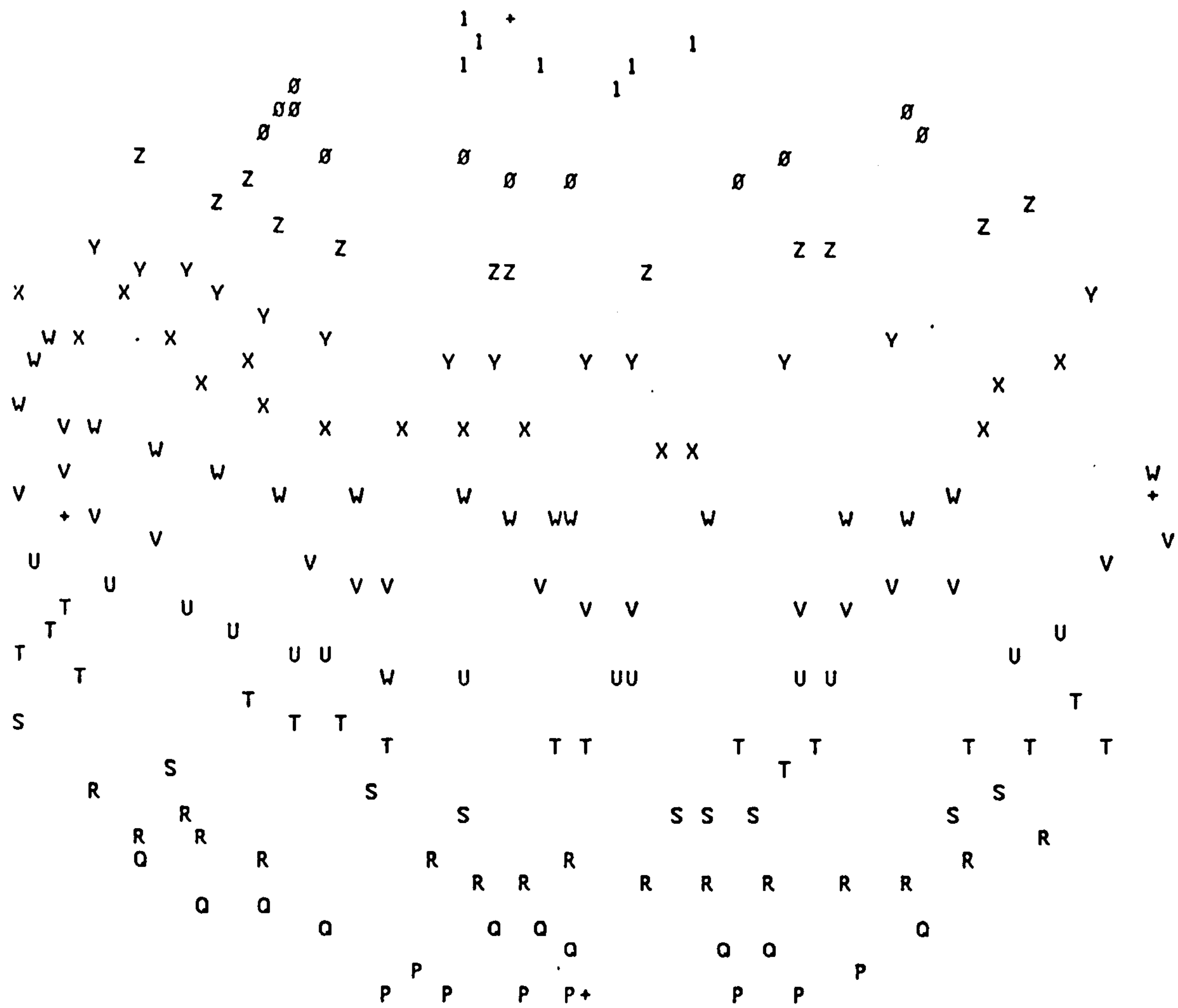

Figure B2.- Computer printout 2.

FRINGE ****** TECHNICAL PAPER-- SANDOR NAGY 17-JUL-86 12:46:57

WAVEFRON DEVIATION IN UNITS OF WAVES
TILT AND DEFOCUS MEASURED FROM DIFFRACTION FOCUS
WAVELENGTH Ø.633 MICRONS

	N	RMS
RAW	Ø	1.676
PLANE	2	Ø.247
SPHERE	3	Ø.115
4H ORDER	8	Ø.1Ø7
6H ORDER	15	Ø.Ø98
8H ORDER	24	Ø.Ø88
COMPLETE	36	Ø.Ø86

STREHL RATIO Ø.592 AT DIFFRACTION FOCUS

FOURTH ORDER ABERRATIONS

MAGNITUDE WAVES	ANGLE DEG	DESIGNATION
3.136	-94.8	TILT
Ø.687		DEFOCUS
Ø.Ø83	Ø.3	ASTIGMATISM
Ø.138	-161.2	COMA
Ø.354		SPHERICAL ABERRATION

FOLLOWING TERMS WERE SUBTRACTED FROM DATA-

TILT FOCUS

RESIDUAL WAVEFRON VARIATIONS EVALUATED AT DATA POINTS

PTS	RMS	MAX	MIN	SPAN	STREHL
169	Ø.118	Ø.368	-1.Ø94	1.463	Ø.575

RESIDUAL WAVEFRON VARIATIONS OVER UNIFORM GRID

PTS	RMS	MAX	MIN	SPAN	STREHL
652.	Ø.Ø61	Ø.258	-Ø.144	Ø.4Ø2	Ø.863

FRINGE ****** TECHNICAL PAPER-- SANDOR NAGY

RMS CALCULATED FROM ZERNIKE COEFFICIENTS=Ø.Ø64

Figure B3.- Computer printout 3.

```
FRINGE ****** TECHNICAL PAPER-- SANDOR NAGY                  17-JUL-86 12:47:00

CONTOUR STEP    WIDTH  PAGE SIZE      -M-       -N-       -P-       -Q-
      0.100     0.800      2.000   -0.150    -0.050     0.050     0.150
+        +        ++        +        11+        +        ++        +        +

                        NNN    MMMM     NNNNNNNN PP
                   NNN MMMMMMMMMMMMMMMM    NNNNNNN PPP
                   N MMMMMMMMMMMMMMMM    NNNNNNNNNNN P
+                NN MMMMMMMMMMMMM      NNNNNNNNNNNNNNN  P                 +
+           P NNNN  MMMMMMM      NNNNNNNNNNNNNNNNNNNNN  PPPPP             +
             NNNNNN       NNNNNNNNNNNNNNNNNNNNNNN      PPPPPP
         PP NNNNNNNNNNNNNNNNNNNNNNNNNNNNNNN      PPPPPPPPPPPPP
         PP NNNNNNNNNNNNNNNNNNNNNNNNNNNNNNN   PPPPPPPPPPPPPPPPPP
         PP  NNNNNNNNNNNNNNNNNNNNNNNNNNNNN   PPPPPPPPPPPPPPPPPP
+      PPPPPP        NNNNNNNNNNNNNNNNNNNNNN   PPPPPPPPPPPPPPPPPP          +
     QQ PPPPPPPPPPPPP    NNNNNNNNNNNNNNNNNNNN   PPPPPPPPPPPPPP
     QQPPPPPPPPPPPPPPPPP   NNNNNNNNNNNNNNNNNNN    PPPPPPPPPPPP
     Q PPPPPPPPPPPPPPPPPP    NNNNNNNNNNNNNNNNNN    PPPPPPPPPPP
   RQ PPPPPPPPPPPPPPPPPPPP                          PPPPPPPPPP    QQQ   P
+  QQ PPPPPP  PPPPPPPPPPPPPPPPPPPPPPPPPPP              PPPPPPPPP   QQQQ  P  +
+  QQPPPPP      PPPPPPPPPPPPPPP                           PPPPPPPPP    Q   P  +
   Q PPPP       PPPPPPPPPPPPP                              PPPPPPPPP       P
    PPPPP       PPPPPPPPPPPPP                  P            PPPPPPPPP     PP
   PPPPPPP    PPPPPPPPPPPPPPP                  PP            PPPPPPPPPPPPPPP
   PPPPPPPPPPPPPPPPPPP PPPPP                   PPP            PPPPPPPPPPPPPP  2
+  PPPPPPPPPPPPPPPP       PP                   PPP             PPPPPPPPPPPPP  +
4  PPPPPPPPPPPPPPP  NNNNNN                     PPPP             PPPPPPPPPPPPP
   PPPPPPPPPPPPP  NNNNNNNNNN                   PPPP               PPPPPPPPPP
   PP PPPPPPPPP  NNNNNNNNNNN                   PPPP
   P N  PPPPPP  NNNNNN   NNN                   PPP        NNN          NNNNN
+  P NNN        NNNNN   MMM  NN              PPPPP        NNNNNNNNNNNNNNNN  +
+  P NNNNN     NNNNNN MMMMMMMM  NNNNNN  PPPPPPPPPPP       NNNNNNNNNNNNNNNN  +
   P NNNNNNNNNNNNNNNN MMMMMMMMMM NNNNNNN   PPPPPPP       NNNNNNNNNNNNNNNNN
     NNNNNNNNNNNNNNN  MMMMMMMMMMM  NNNNNNN    PPPPP      NNNNNNNNNNNNNNN
     NNNNNNNNNNNNNNNN  MMMMMMMMM  NNNNNNNN    PPPPP      NNNNNNNNNN  NNN
     P NNNNNNNNNNNNNNNN  MMMMMM   NNNNNNNN   PPPPPP      NNNNNNN     NNN
+       NNNNNNNNNNNNNNNNNNN  NNNNNNNNNNN   PPPPPPPPP  NNNNNNN     N         +
          NNNNNNNNNNNNNNNNNNNNNNNNNNNNN   PPPPPPPPPP  NNNNNN   M
          NNNNNNN         NNNNNNNN   PPPPPPPPPPPPPP  NNNNN  MMM N
            NNNNN   PPPPPPPPPPPPPPPPPPPPPPPPPPPPPPP  NNNNN     NNN
             NNNN   PPPPPPPPPPPPPPPPPPPPPPPPPPPPPP  NNNNN    NN
+            P NN   PPPPPPPPPPPPPPPPPPPPPPPPPPPPP NNNNNNN  NNN                +
+                     PPPPPPPPPPPPPPPPPPPPPPPPP  NNNNNNNNN                    +
                    PPPPPPPPPPPPPPPPPPPPPPPP  NNNNNNNNN
                    PPPPPPPPPPPPPPPPPPPPP   NNNNNNNNNPP
                         PPPPPPPPPPPPPPP          PP

+        +        ++        +        +33        +        ++        +        +

ZERNIKE POLYNOMIAL COEFFICIENTS

    0.0000    0.0000    0.0000    0.0541    0.0277   -0.0290   -0.0120    0.0349
   -0.0267    0.1010   -0.0141    0.0221   -0.0015    0.0352   -0.0096    0.0219
   -0.0208    0.0117   -0.0473   -0.0066   -0.0629   -0.0176    0.0040    0.0766
    0.0044    0.0207   -0.0214    0.0012   -0.0492   -0.0035   -0.0155    0.0119
   -0.0182   -0.0213   -0.0104    0.0028

RESIDUAL   WAVEFRON VARIATIONS OVER UNIFORM MESH



       PTS       RMS       MAX       MIN      SPAN     VOLUM
      652.     0.061     0.258    -0.144     0.402     0.418
END OF DATA
```

Figure B4.- Computer printout 4.

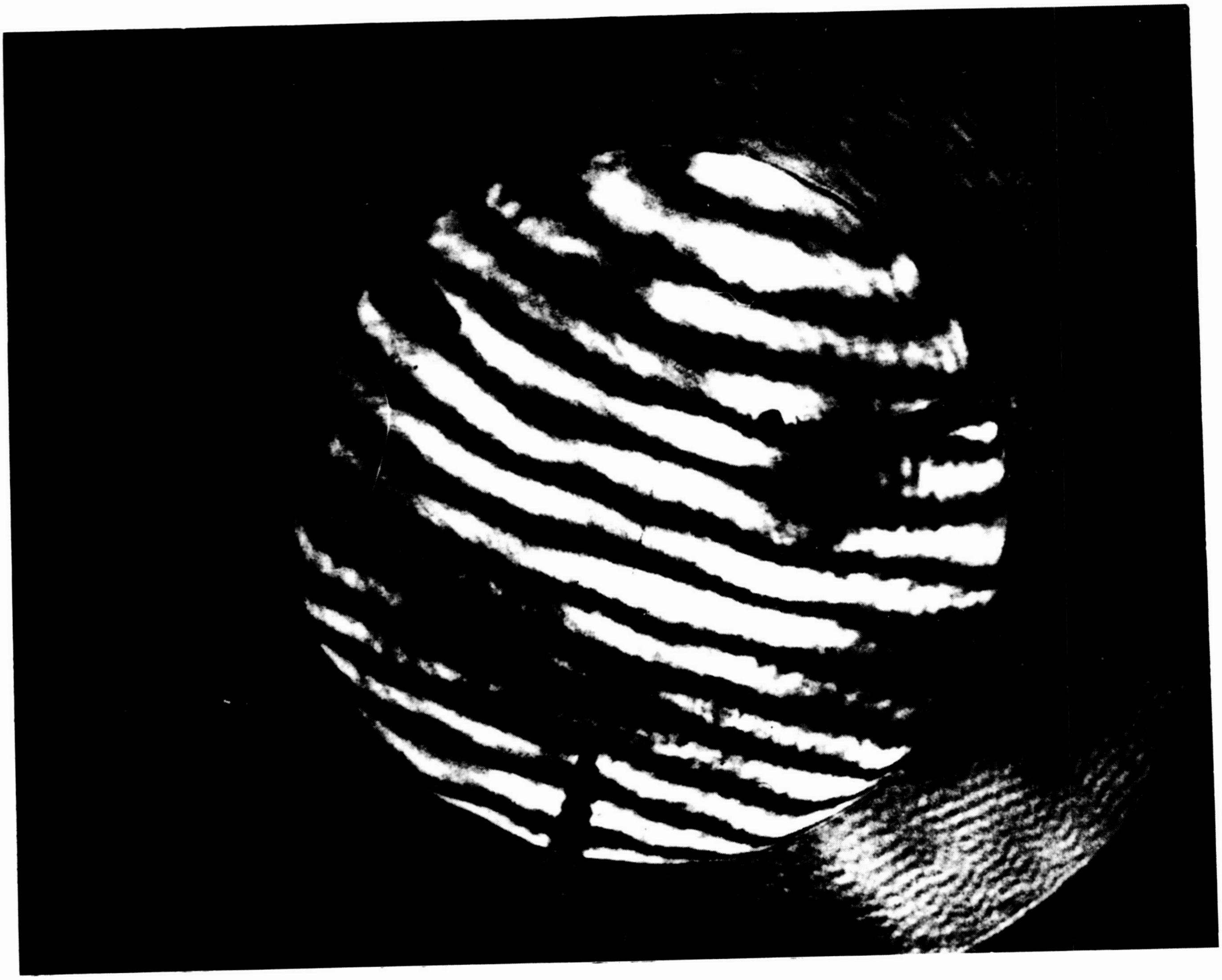

Figure C1.- Interference fringe pattern.

ORIGINAL PAGE
BLACK AND WHITE PHOTOGRAPH

ORIGINAL PAGE
BLACK AND WHITE PHOTOGRAPH

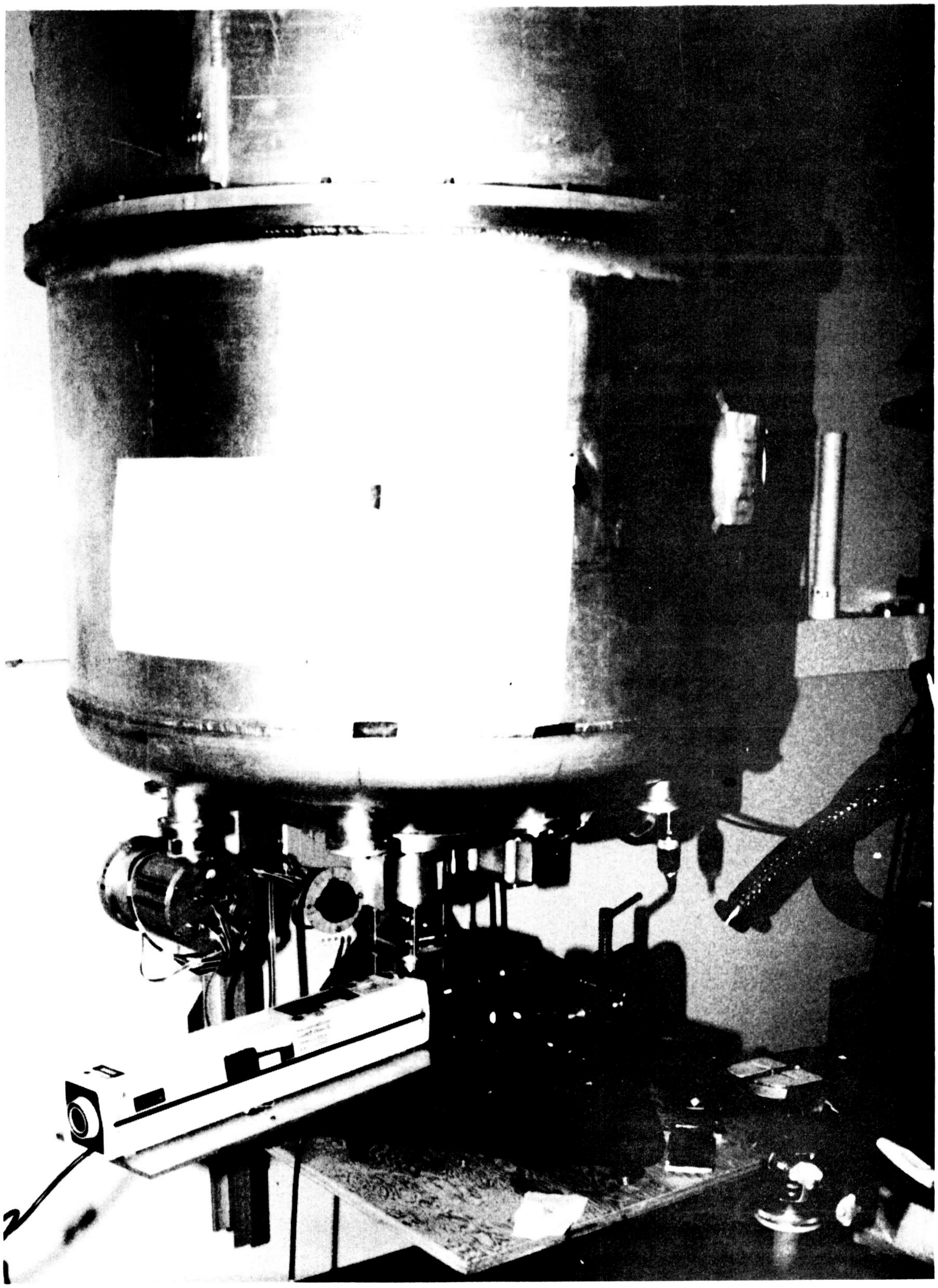

Figure C2.- Laser Interferometer with bottom of dewar.

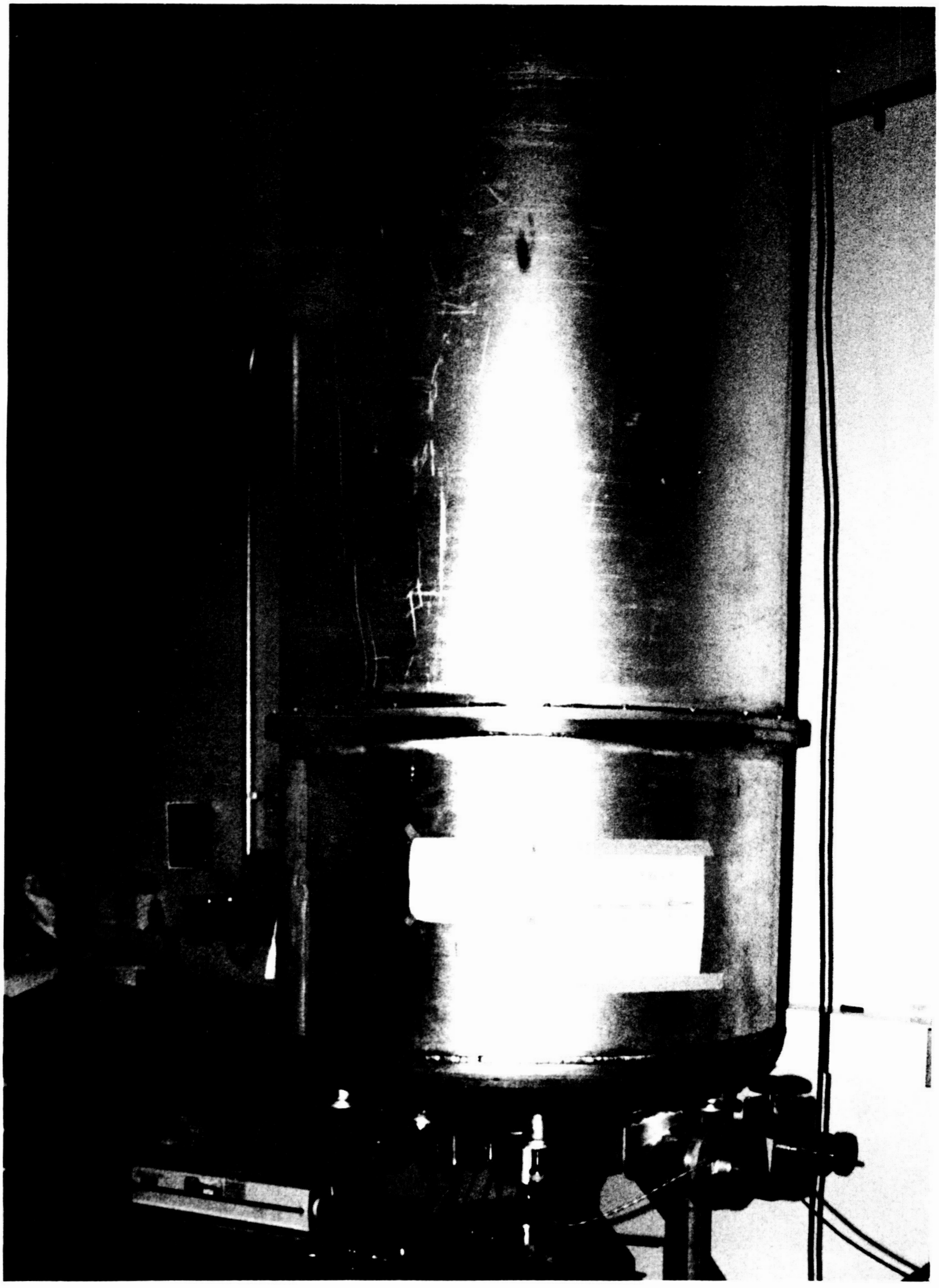

Figure C3.- Dewar assembly.

ORIGINAL PAGE
BLACK AND WHITE PHOTOGRAPH

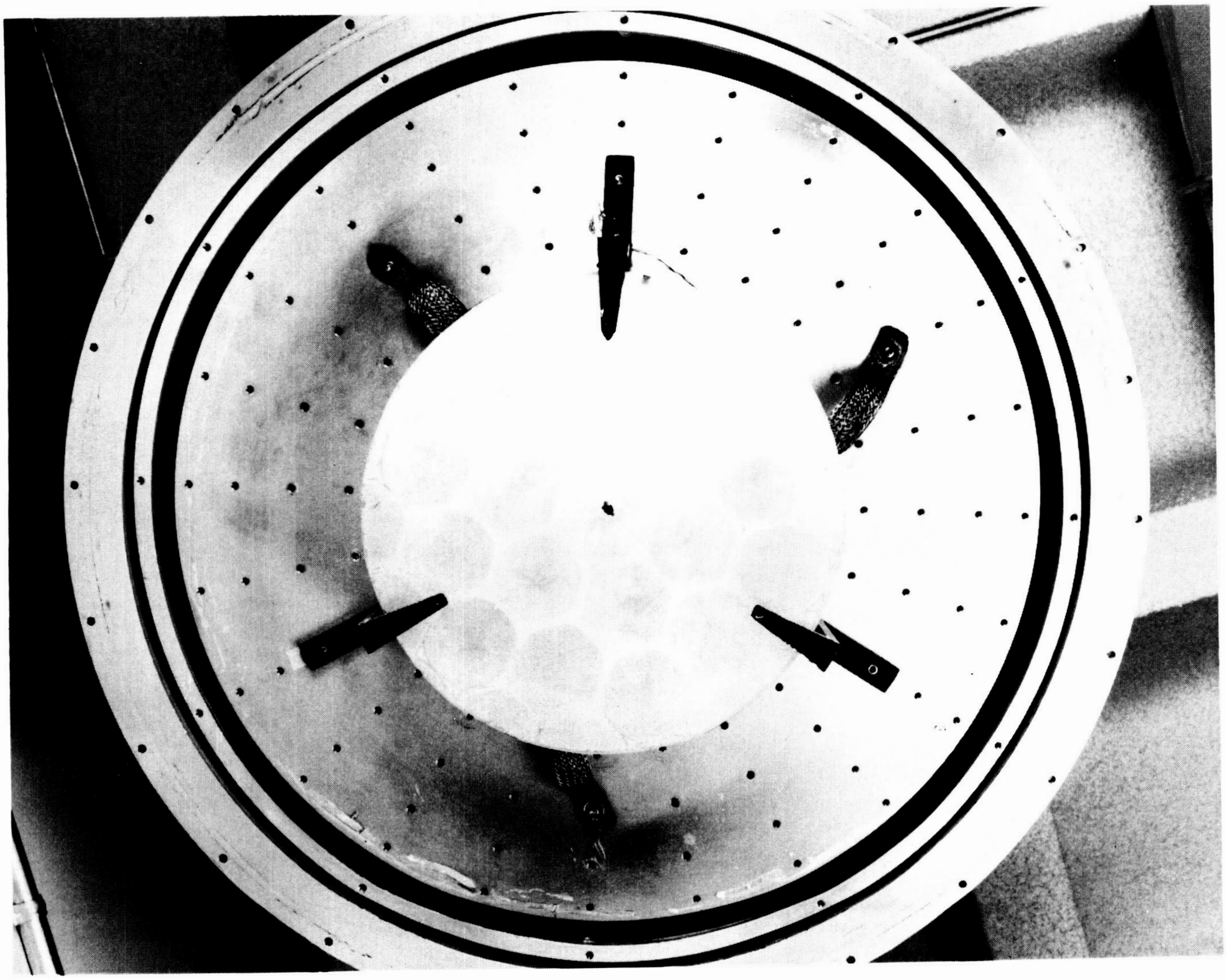

Figure C4.- Pyrex Hexcore Mirror 1A mounted to bottom of dewar assembly.

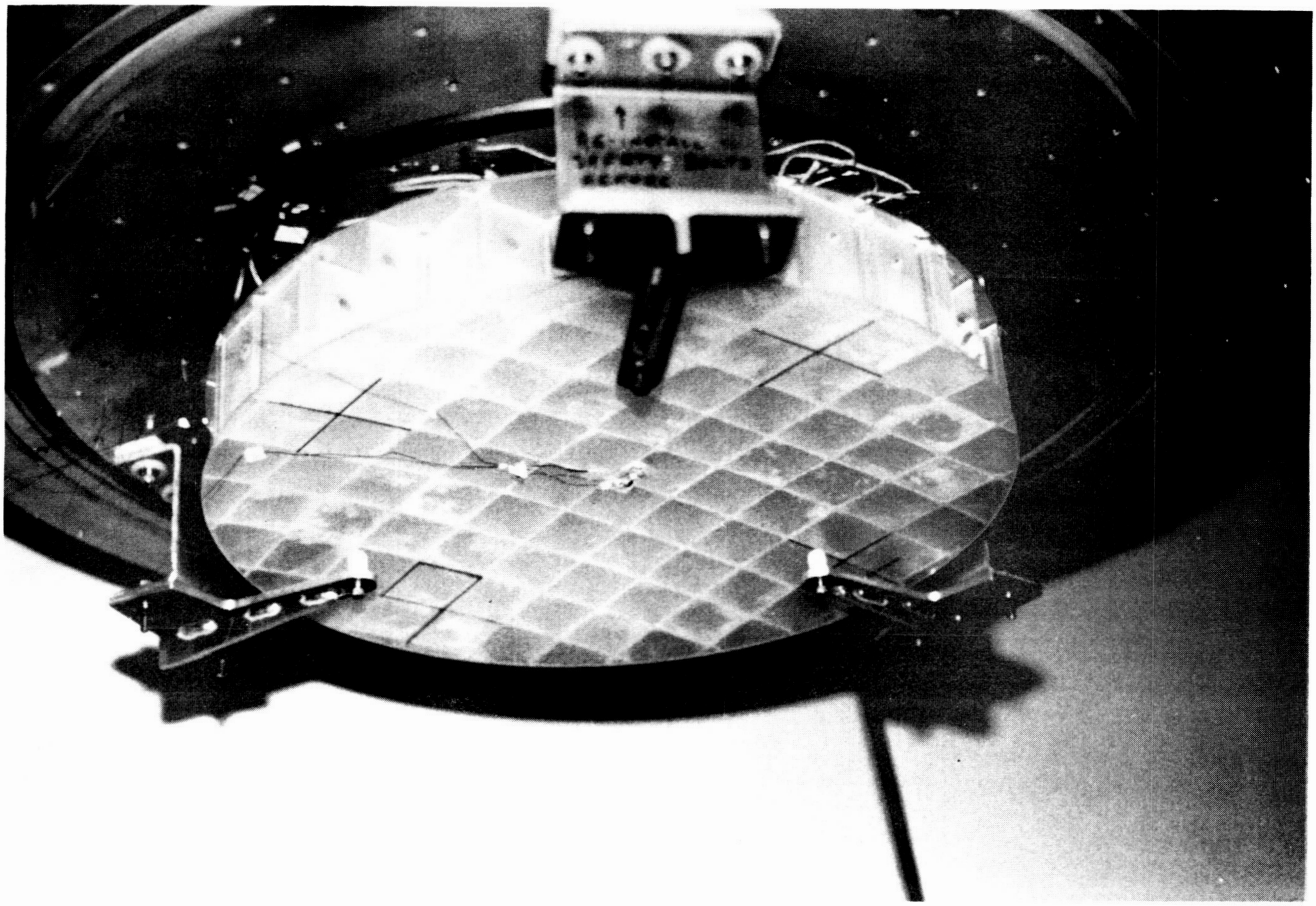

Figure C5.- Fused silica ultralightweight frit-bonded mirror.

ORIGINAL PAGE
BLACK AND WHITE PHOTOGRAPH

```
$ TYP FOR025.DAT

FRINGE
VAX
REF
    .0000  .0000  .0000  .0541  .0277 -.0290 -.0120  .0349
   -.0267  .1010 -.0141  .0221 -.0015  .0352 -.0096  .0219
   -.0208  .0117 -.0473 -.0066 -.0629 -.0176  .0040  .0766
    .0044  .0207 -.0214  .0012 -.0492 -.0035 -.0155  .0119
   -.0182 -.0213 -.0104  .0028
POLYNOMI
FIDS 100 200  200 100  100 0  0 100
WEDGE 0.5
STEP .1
WIDTH .4
COBS .25
PART
END
DANA WAMAP PLOT3D END
$ TYP FOR009.DAT
```

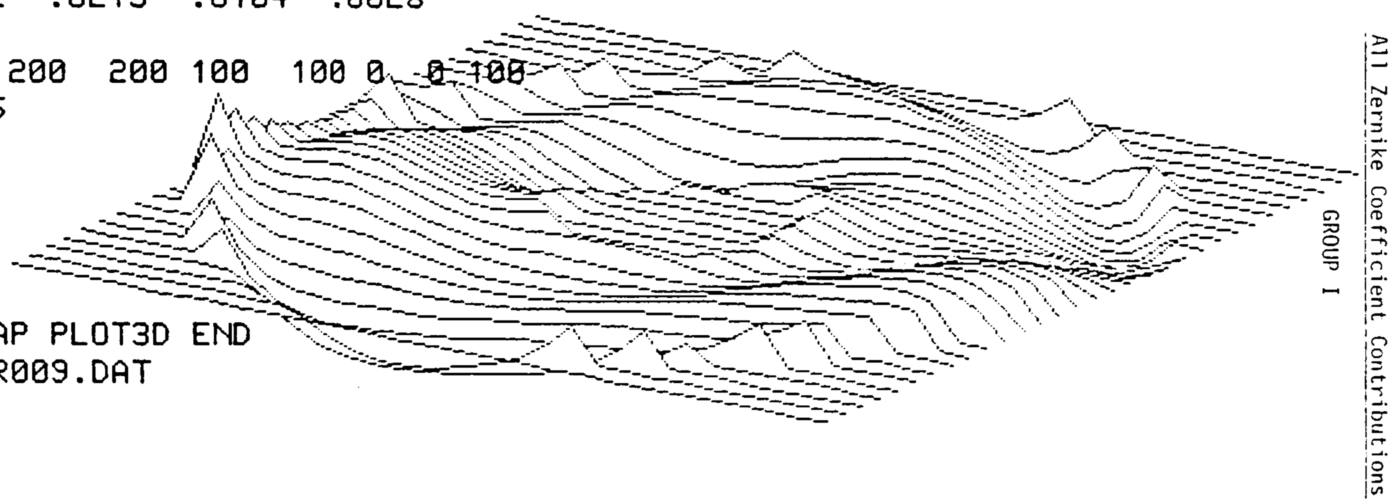

Figure D1.- Plot IA.

```
$ TYP FOR025.DAT
FRINGE
VAX
REF
   .0000    .0000    .0000    .0541    .0277  -.0290  -.0120    .0349
  -.0267    .1010  -.0141    .0221  -.0015    .0352  -.0096    .0219
  -.0208    .0117  -.0473  -.0066  -.0629  -.0176    .0040    .0766
   .0044    .0207  -.0214    .0012  -.0492  -.0035  -.0155    .0119
  -.0182  -.0213  -.0104    .0028
POLYNOMI
FIDS 100 200  200 100  100 0  0 100
PART
END
ESCAN GSPOT ZONE END

$ TYP FOR009.DAT
```

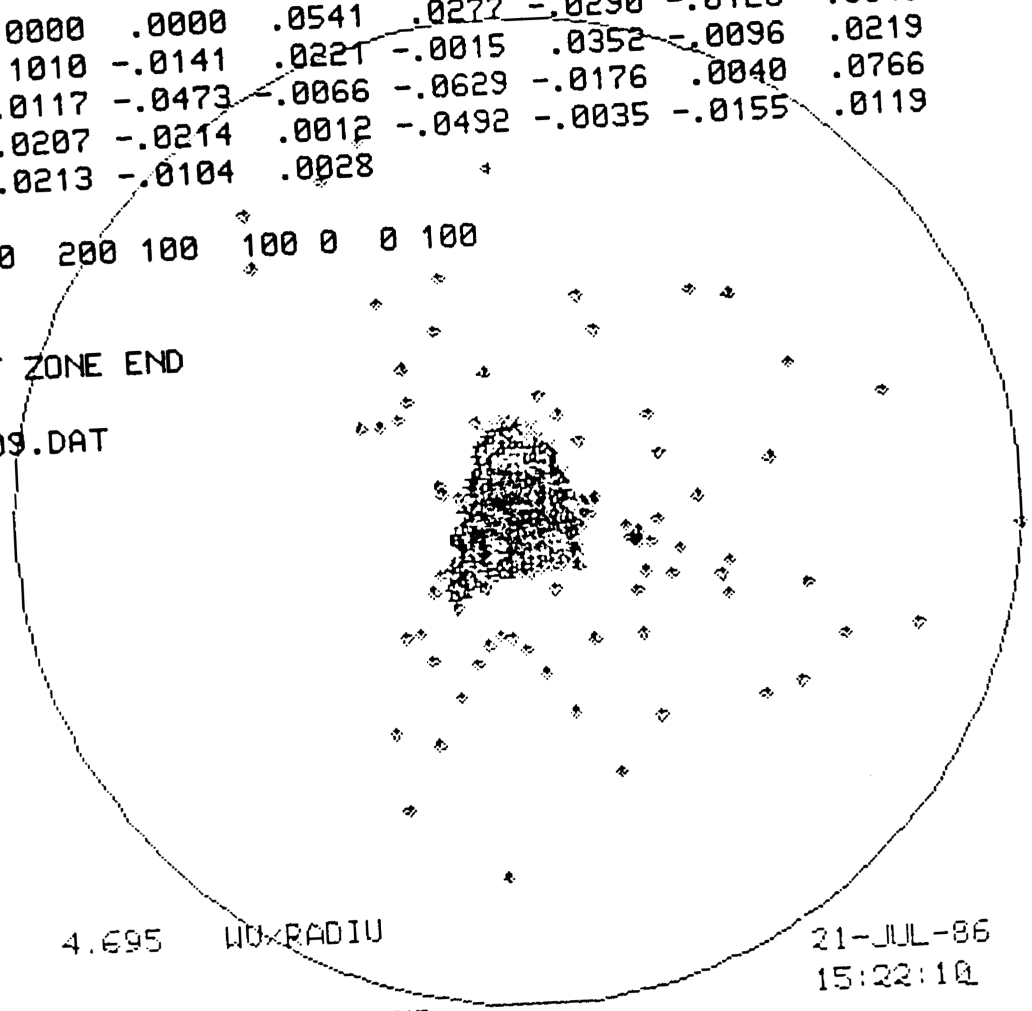

Figure D2.- Plot IB.

IB

ORIGINAL PAGE IS OF POOR QUALITY

ORIGINAL PAGE IS
OF POOR QUALITY

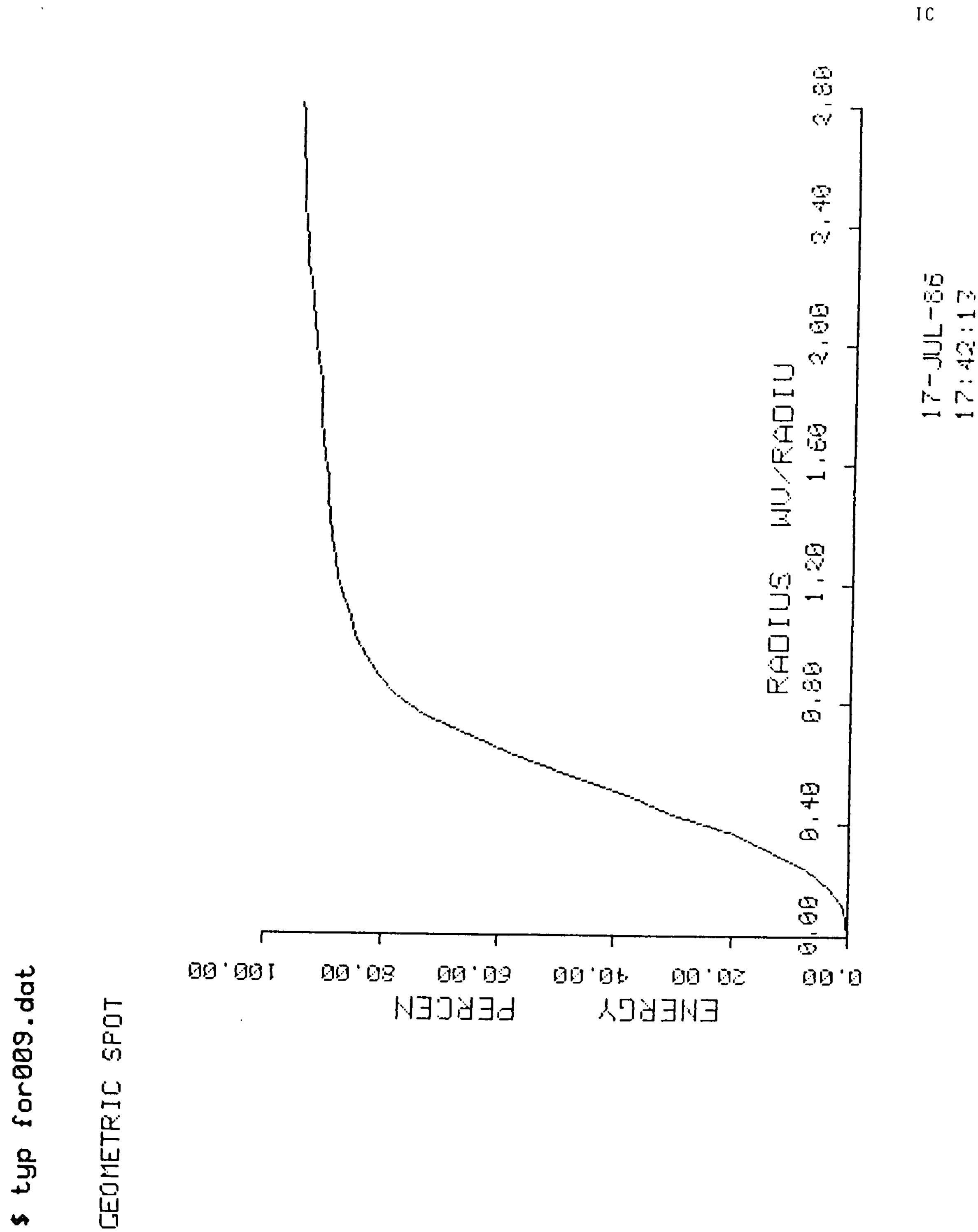

Figure D3.- Plot IC.

Radial Contribution (spherical aberration)

GROUP II

```
*

$ TYP FOR025.DAT

FRINGE
VAX
REF
     .0000  .0000  .0000  .0000  .0000  .0000  .0000  .0349
     .0000  .0000  .0000  .0000  .0000  .0000 -.0096  .0000
     .0000  .0000  .0000  .0000  .0000  .0000  .0000  .0766
     .0000  .0000  .0000  .0000  .0000  .0000  .0000  .0000
     .0000  .0000 -.0104  .0028
POLYNOMI
FIDS 410 528 612 330 412 131 213 332
WEDGE 0.5
STEP .1
WIDTH .4
COBS .25
PART
END
DANA WAMAP PLOT3D END
$ TYP FOR009.DAT
```

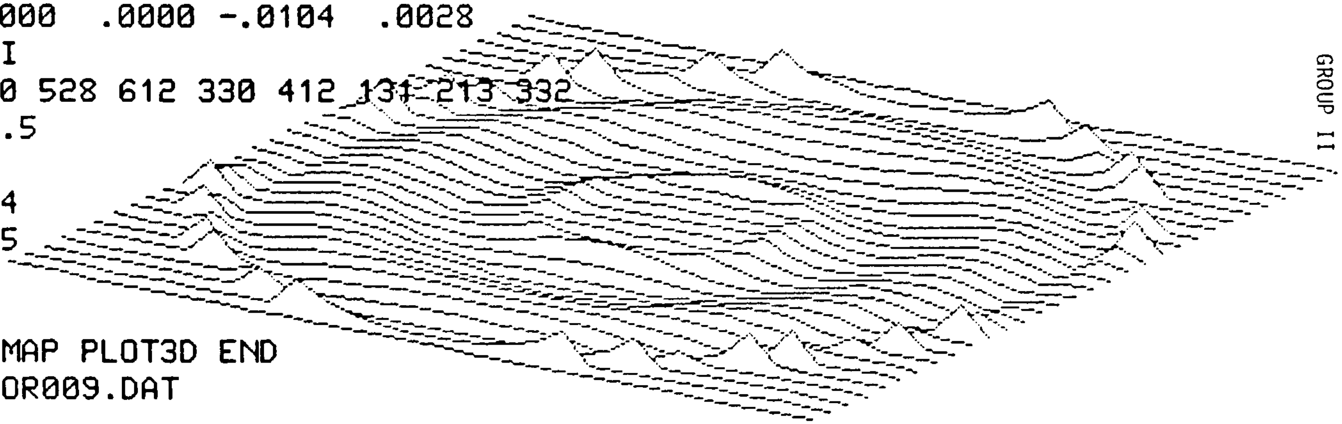

WAVEFRONWAVES   RADIUS

17- III -86

Figure D4.- Plot IIA.

ORIGINAL PAGE IS
OF POOR QUALITY

II B

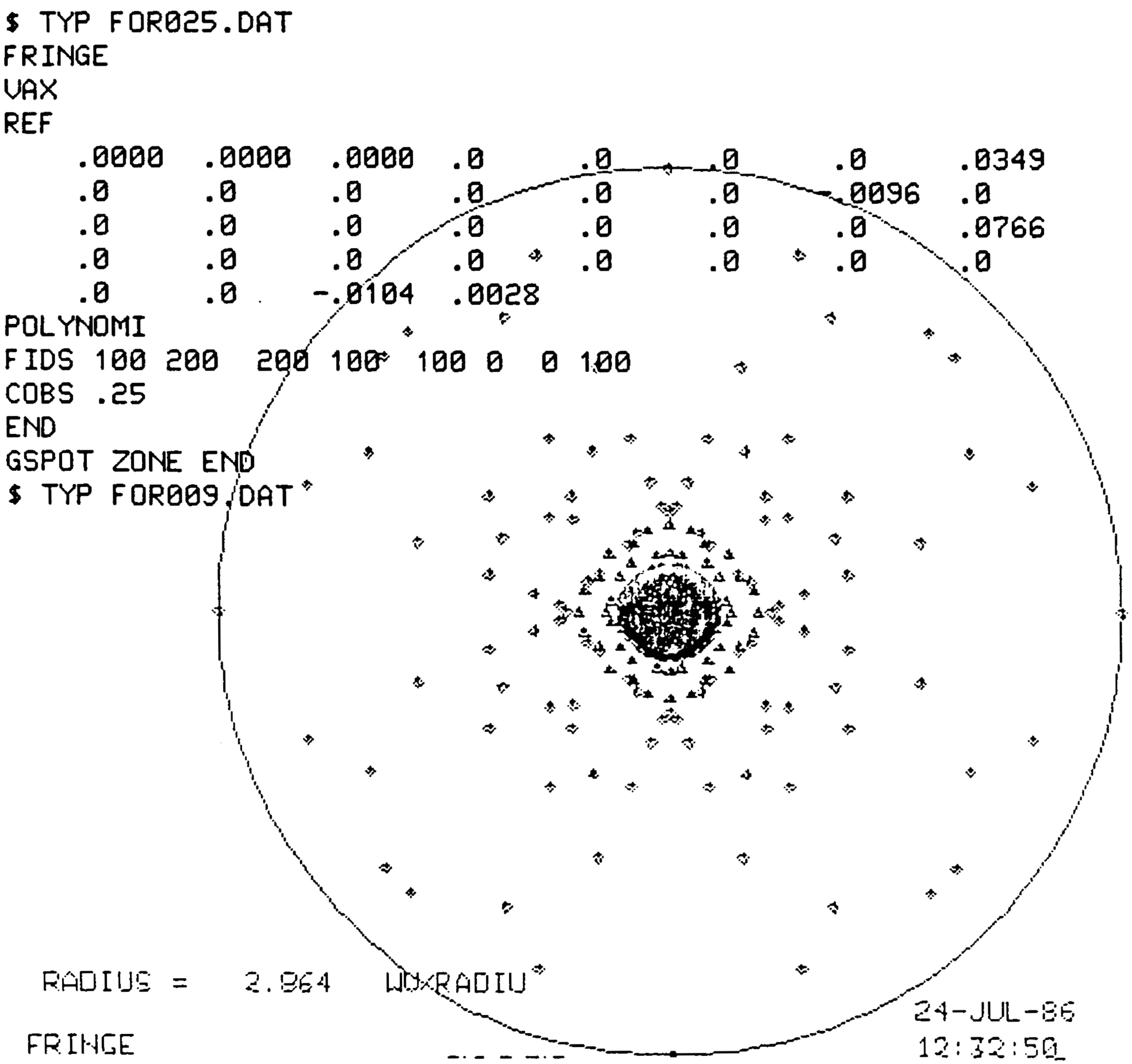

Figure D5.- Plot IIB.

```
$ typ for025.dat
FRINGE
VAX
REF
   GEOMETRIC SPOT
    .0000   .0000   .0000  .0      .0      .0      .0      .0349
    .0      .0      .0     .0      .0      .0    -.0096    .0
    .0      .0      .0     .0      .0      .0      .0      .0766
    .0      .0      .0     .0      .0      .0      .0      .0
    .0      .0      .0104  .0028
POLYNOMI
FIDS 100 200  200 100  100 0  0 100
COBS .25
END
GSPOT RED END
$ typ for009.dat
```

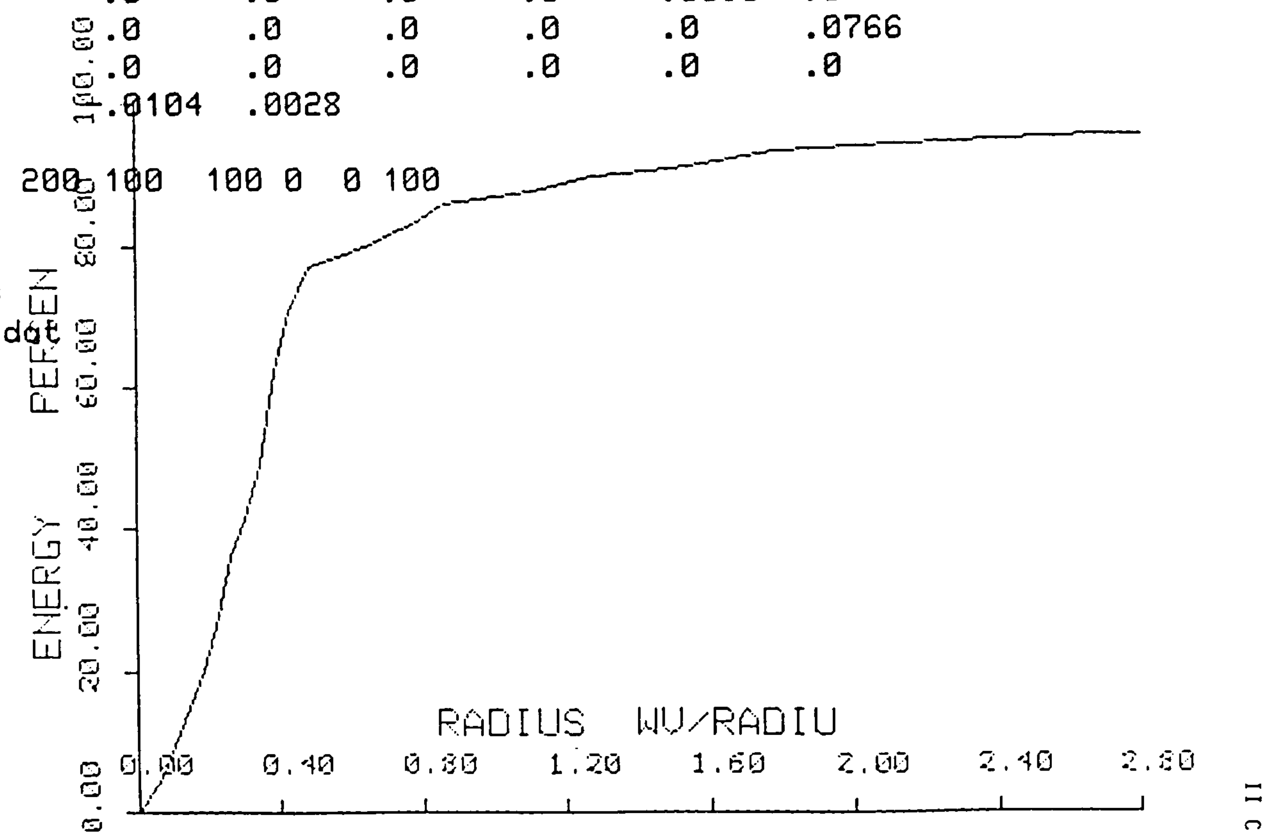

Figure D6.- Plot IIC.

ORIGINAL PAGE IS OF POOR QUALITY

```
*

$ TYP FOR025.DAT

FRINGE
VAX
REF
      .0000   .0000   .0000   .0000   .0000 -.0290 -.0120   .0000
      .0000   .0000   .0000   .0000 -.0015   .0352   .0000   .0000
      .0000   .0000   .0000   .0000   .0000 -.0176   .0040   .0000
      .0000   .0000   .0000   .0000   .0000   .0000   .0000   .0000
     -.0182 -.0213   .0000   .0000
POLYNOMI
FIDS 410 528 612 330 412 131 213 332
WEDGE 0.5
STEP .1
WIDTH .4
COBS .25
PART
END
DANA WAMAP PLOT3D END
$ TYP FOR009.DAT
```

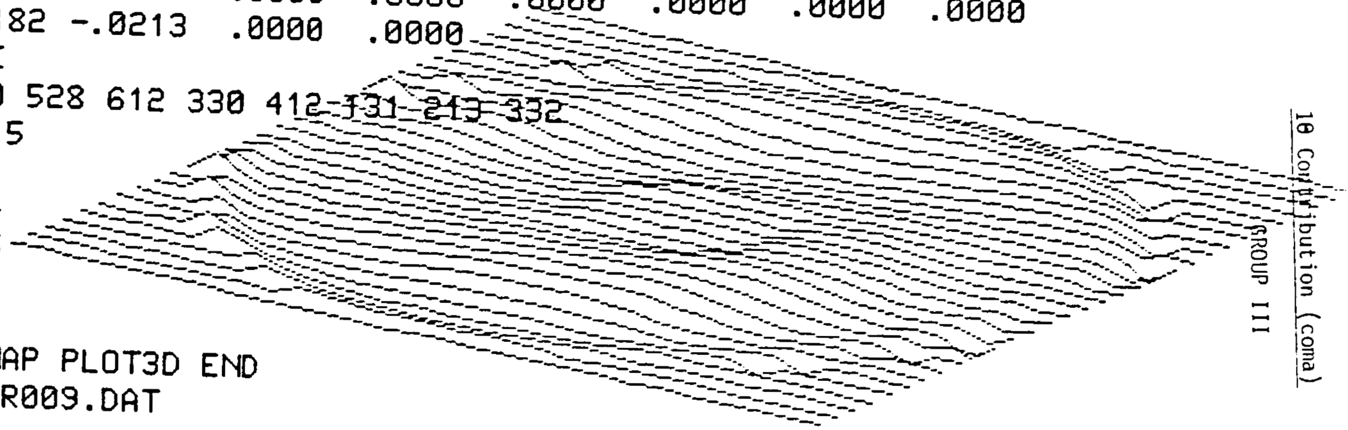

Figure D7.- Plot IIIA.

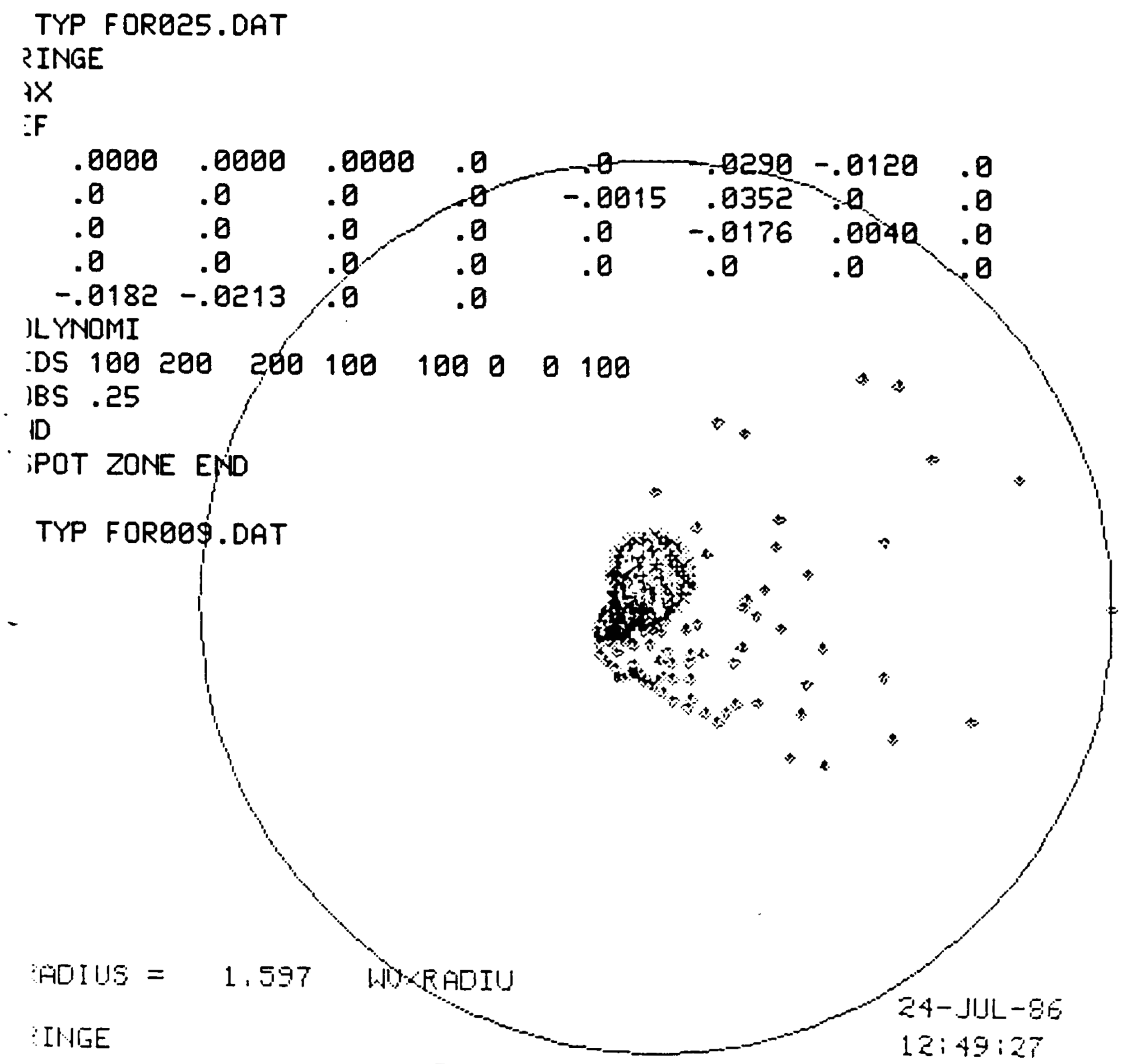

Figure D8.- Plot IIIB.

```
$ TYP FOR025.DAT
FRINGE
VAX
REF
    .0000   .0000   .0000   .0      .0      -.0290  -.0120  .0
    .0      .0      .0      .0      -.0015  .0352   .0      .0
    .0      .0      .0      .0      .0      -.0176  .0040   .0
    .0      .0      .0      .0      .0      .0      .0      .0
   -.0182  -.0213   .0      .0
POLYNOMI
FIDS 100 200  200 100  100 0  0 100
COBS .25
END
GSPOT RED END

$ TYP FOR009.DAT
```

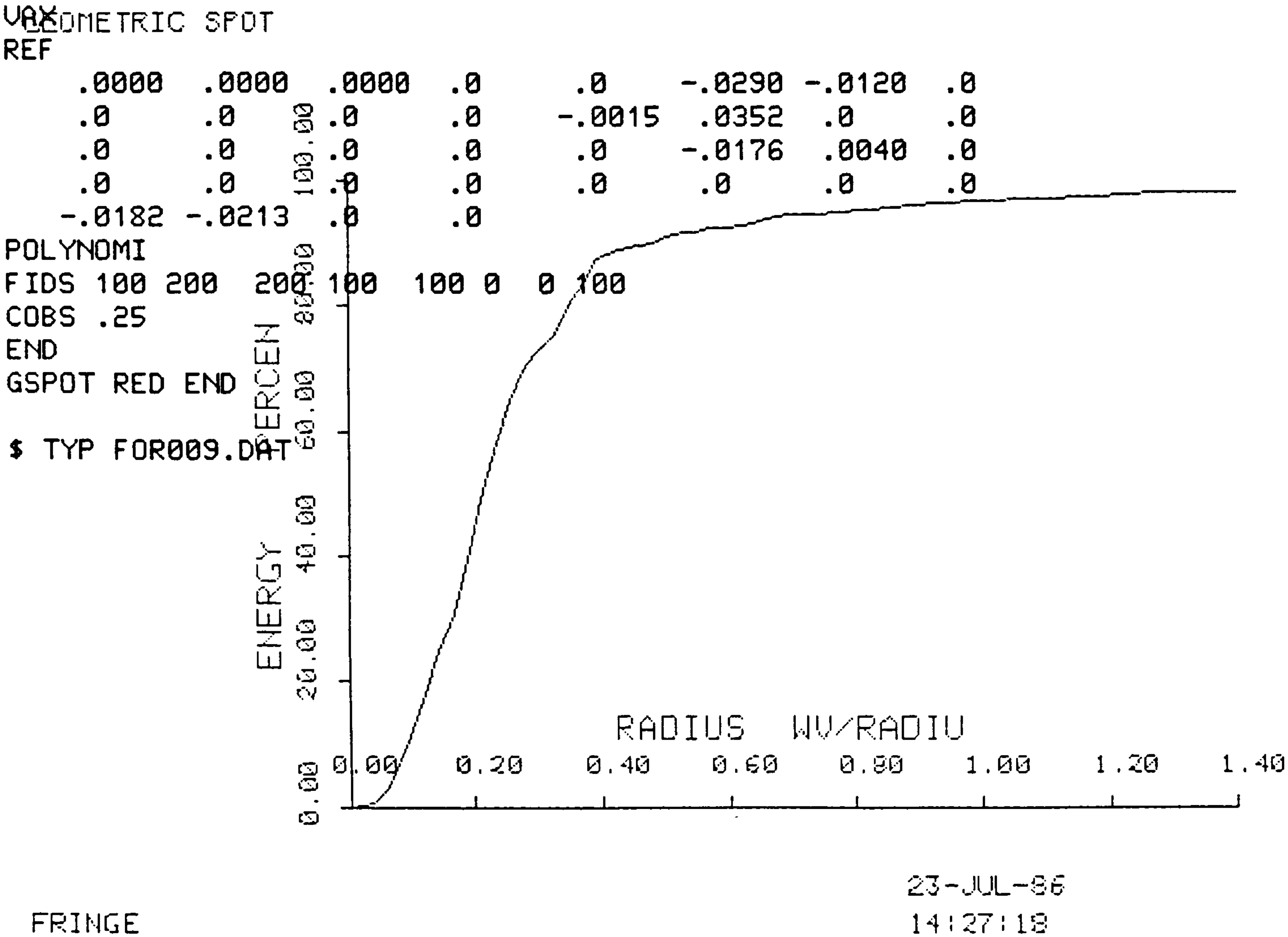

Figure D9.- Plot IIIC.

```
$ TYP FOR025.DAT

FRINGE
VAX
REF
     .0000  .0000  .0000  .0541  .0277  .0000  .0000  .0000
     .0000  .0000 -.0141  .0221  .0000  .0000  .0000  .0000
     .0000  .0000  .0000 -.0066 -.0629  .0000  .0000  .0000
     .0000  .0000  .0000  .0000  .0000  .0000 -.0155  .0119
     .0000  .0000  .0000  .0000
POLYNOMI
FIDS 410 528 612 330 412 131 213 332
WEDGE 0.5
STEP .1
WIDTH .4
COBS .25
PART
END
DANA WAMAP PLOT3D END
$ TYP FOR009.DAT
```

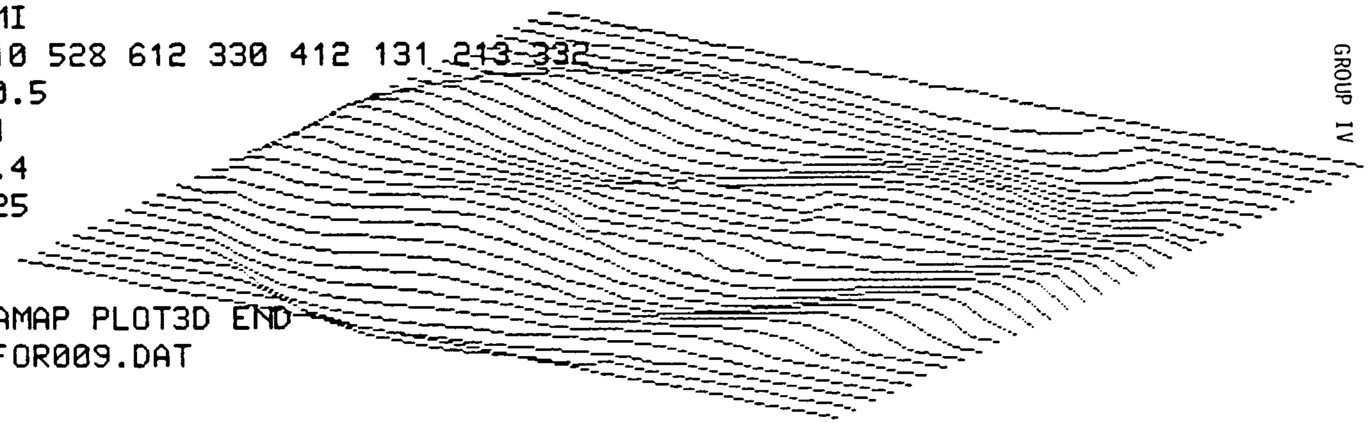

Figure D10.- Plot IVA.

ORIGINAL PAGE IS
OF POOR QUALITY

```
$ TYP FOR025.DAT
FRINGE
VAX
REF
     .0       .0       .0       .0       .0       .0       .0       .0
   -.0267   .1010    .0       .0       .0       .0       .0       .0
     .0     .0117  -.0473     .0       .0       .0       .0       .0
     .0       .0       .0       .0    -.0492  -.0035     .0       .0
     .0       .0       .0       .0
POLYNOMI
FIDS 100 200  200 100  100 0  0 100
COBS .25
END
GSPOT ZONE END

$ TYP FOR009.DAT
```

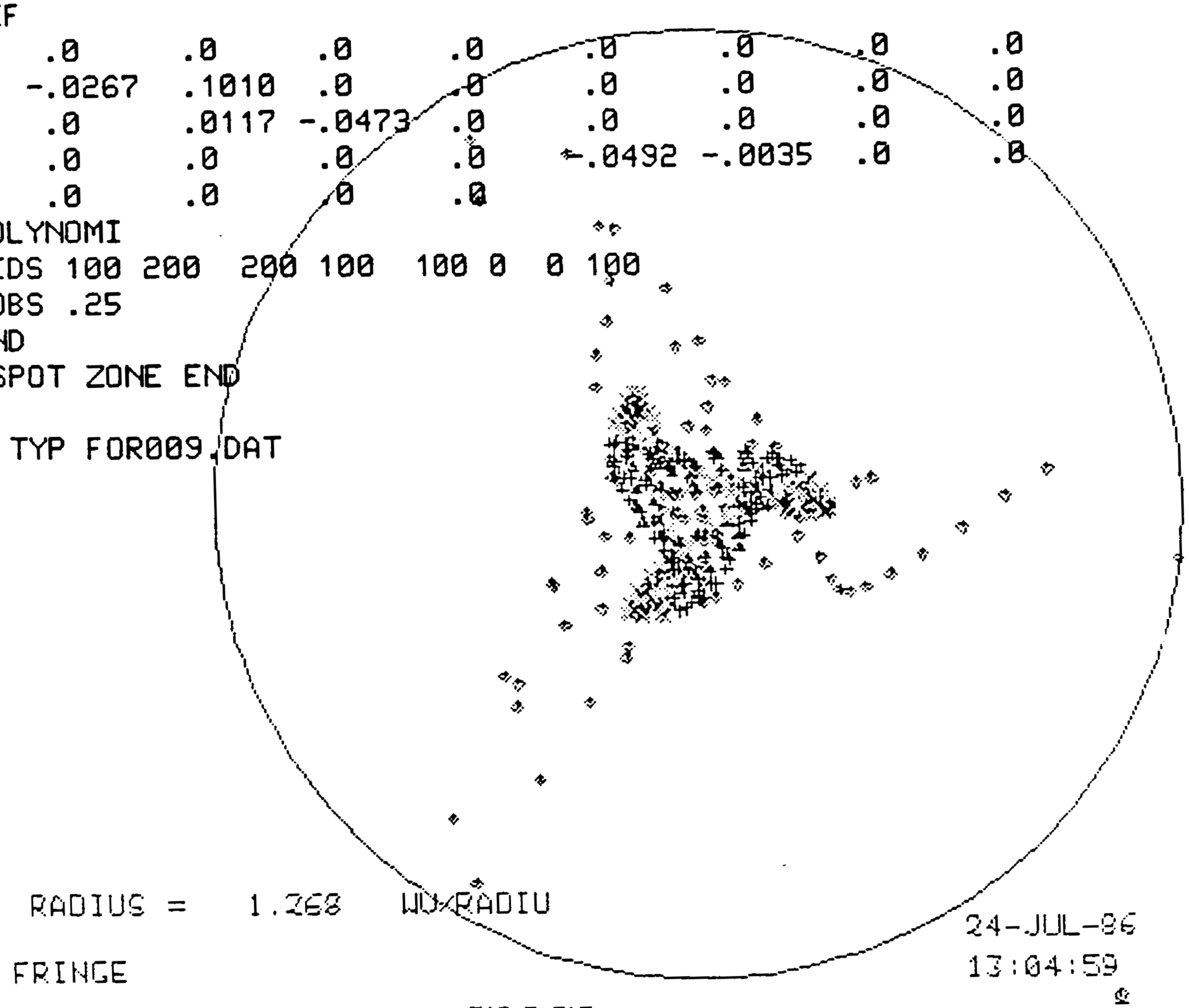

Figure D11.- Plot IVB.

ORIGINAL PAGE IS
OF POOR QUALITY

IV B

```
$ TYP FOR025.DAT
FRINGE
UAX
GEOMETRIC SPOT
REF
    .0000  ..0000   .0000   .0541   .0277   .0     .0      .0
    .0      .0     -.0141   .0221   .0      .0     .0      .0
    .0      .0      .0     -.0066  -.0629   .0     .0      .0
    .0      .0      .0      .0      .0      .0    -.0155   .0119
    .0      .0      .0      .0
POLYNOMI
FIDS 100 200  200 100  100 0  0 100
COBS .25
END
GSPOT RED END

$ TYP FOR009.DAT
```

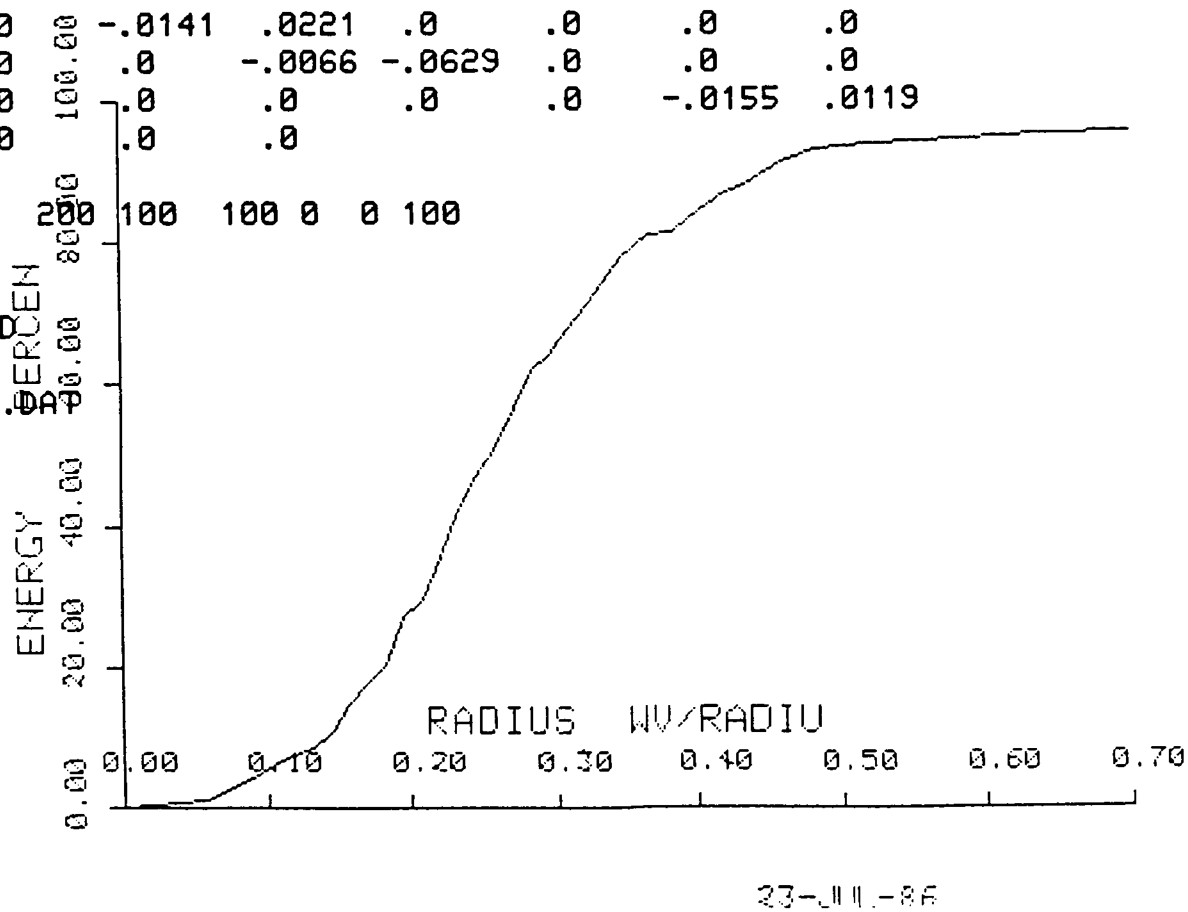

IV C

Figure D12.- Plot IVC.

ORIGINAL PAGE IS
OF POOR QUALITY

```
$ TYP FOR025.DAT

FRINGE
VAX
REF
      .0000   .0008   .0000   .0000   .0000   .0000   .0000   .0000
     -.0267   .1018   .0000   .0000   .0000   .0000   .0000   .0000
      .0000   .0117  -.0473   .0000   .0000   .0000   .0000   .0000
      .0000   .0000   .0000   .0000  -.0492  -.0035   .0000   .0000
      .0000   .0000   .0000   .0000
POLYNOMI
FIDS 410 523 612 330 412 131 213 332
WEDGE 0.5
STEP .1
WIDTH .4
COBS .25
PART
END
DANA WAMAP PLOT3D END
$ TYP FOR009.DAT
```

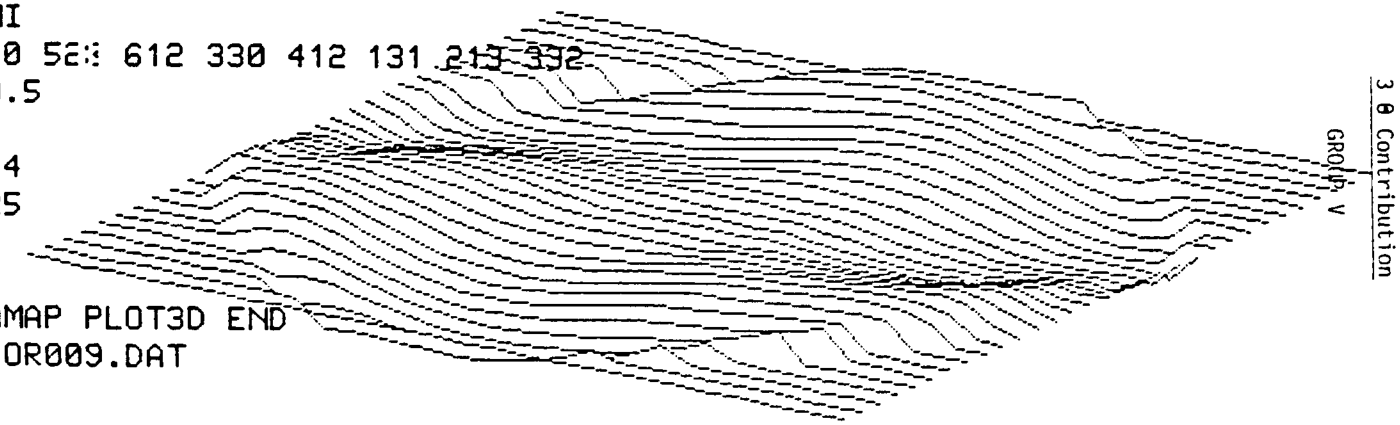

ORIGINAL PAGE IS
OF POOR QUALITY

V A

WAVEFRONWAVES   RADIUS

17-JUL-86
14:45:34

Figure D13.- Plot VA.

```
$ TYP FOR025.DAT
FRINGE
VAX
REF
    .0000   .0000   .0000   .0541   .0277   .0      .0      .0
    .0      .0     -.0141   .0221   .0      .0      .0      .0
    .0      .0      .0     -.0066  -.0629   .0      .0      .0
    .0      .0      .0      .0      .0      .0     -.0155   .0119
    .0      .0      .0      .0
POLYNOMI
FIDS 100 200  200 100  100 0  0 100
COBS .25
END
GSPOT ZONE END

$ TYP FOR009.DAT
```

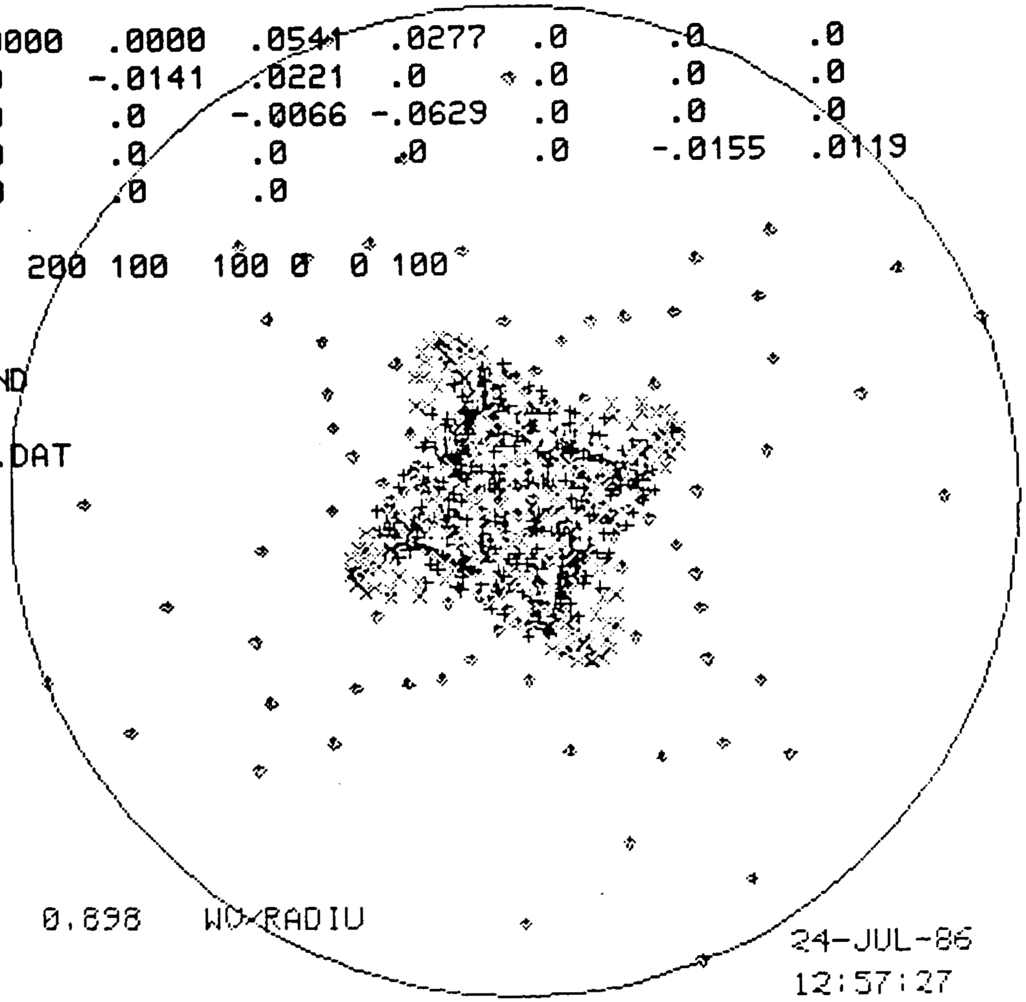

Figure D14.- Plot VB.

ORIGINAL PAGE IS
OF POOR QUALITY

```
$ TYP FOR025.DAT
FRINGE
VAX
REF
    .0      .0      .0      .0      .0      .0      .0      .0
   -.0267   .1010   .0      .0      .0      .0      .0      .0
    .0      .0117  -.0473   .0      .0      .0      .0      .0
    .0      .0      .0      .0     -.0492  -.0035   .0      .0
    .0      .0      .0      .0
POLYNOMI
FIDS 100 200  200 100  100 0  0 100
COBS .25
END
GSPOT RED END

$ TYP FOR009.DAT
```

GEOMETRIC SPOT

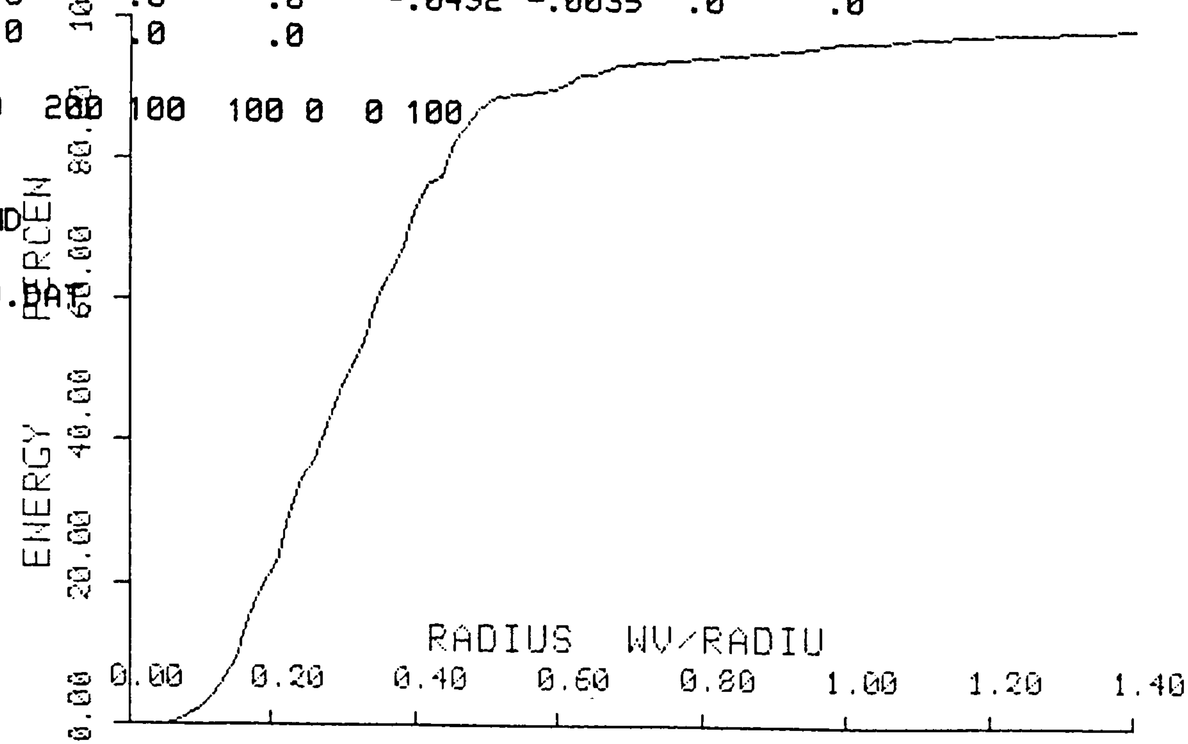

V C

24-JUL-86

FRINGE

Figure D15.- Plot VC.

```
TYP FOR025.DAT

FRINGE
VAX
REF
      .0000   .0000   .0000   .0000   .0000   .0000   .0000   .0000
      .0000   .0000   .0000   .0000   .0000   .0000   .0000   .0219
     -.0208   .0000   .0000   .0000   .0000   .0000   .0000   .0000
      .0000   .0000  -.0214   .0012   .0000   .0000   .0000   .0000
      .0000   .0000   .0000   .0000
POLYNOMI
FIDS 410 528 612 330 412 131 213 332
WEDGE 0.5
STEP .1
WIDTH .4
COBS .25
PART
END
DANA WAMAP PLOT3D END
$ TYP FOR009.DAT
```

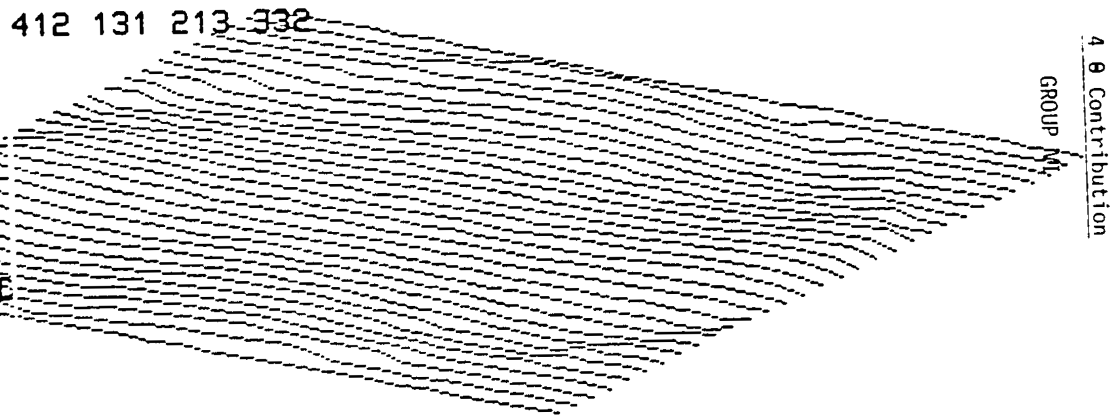

VI A

WAVEFRONWAVES   RADIUS

17-JUL-86
14:57:31

Figure D16.- Plot VIA.

```
$ TYP FOR025.DAT
FRINGE
VAX
REF
    .0      .0      .0      .0      .0      .0      .0      .0
    .0      .0      .0      .0      .0      .0      .0      .0219
  -.0208    .0      .0      .0      .0      .0      .0      .0
    .0      .0    -.0214  .0012    .0      .0      .0      .0
    .0      .0      .0      .0
POLYNOMI
FIDS 100 200  200 100  100 0  0.100
COBS .25
END
GSPOT ZONE END

$ TYP FOR009.DAT
```

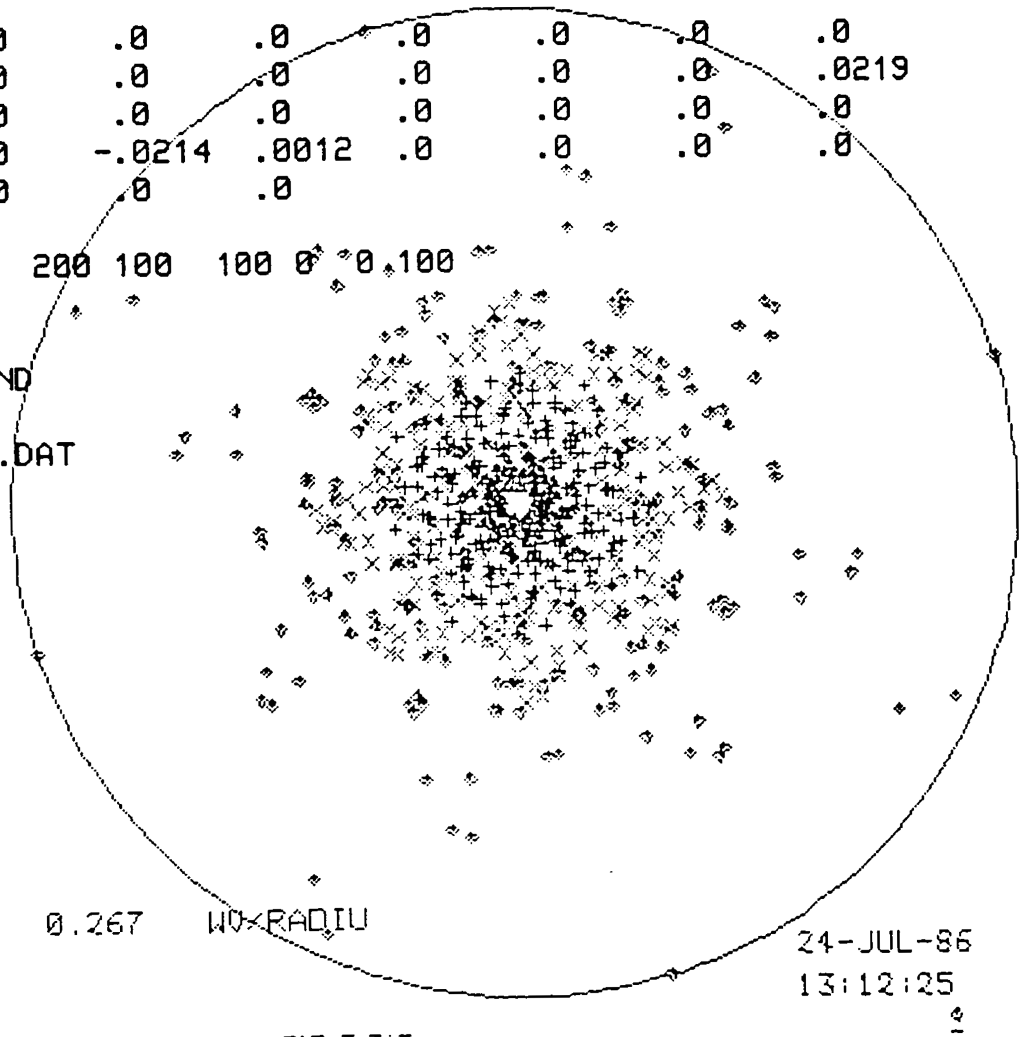

Figure D17.- Plot VIB.

```
$ TYP FOR025.DAT
FRINGE
VAX GEOMETRIC SPOT
REF
    .0       .0      .0      .0      .0      .0      .0      .0
    .0       .0      .0      .0      .0      .0      .0      .0219
   -.0208    .0      .0      .0      .0      .0      .0      .0
    .0       .0      .0214   .0012   .0      .0      .0      .0
    .0       .0      .0      .0
POLYNOMI
FIDS 100 200  200 100  100 0  0 100
COBS .25
END
GSPOT RED END

$ TYP FOR009.DAT
```

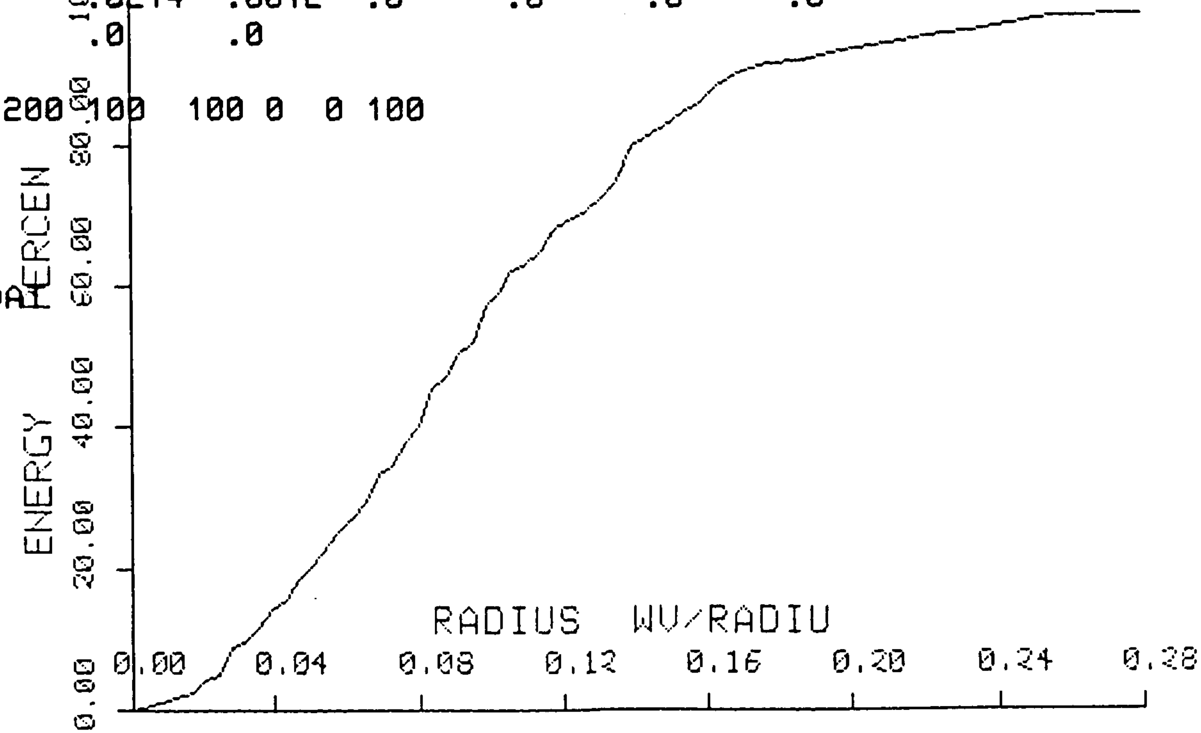

24-JUL-86
12:00:58

FRINGE

VI C

Figure D18.- Plot VIC.

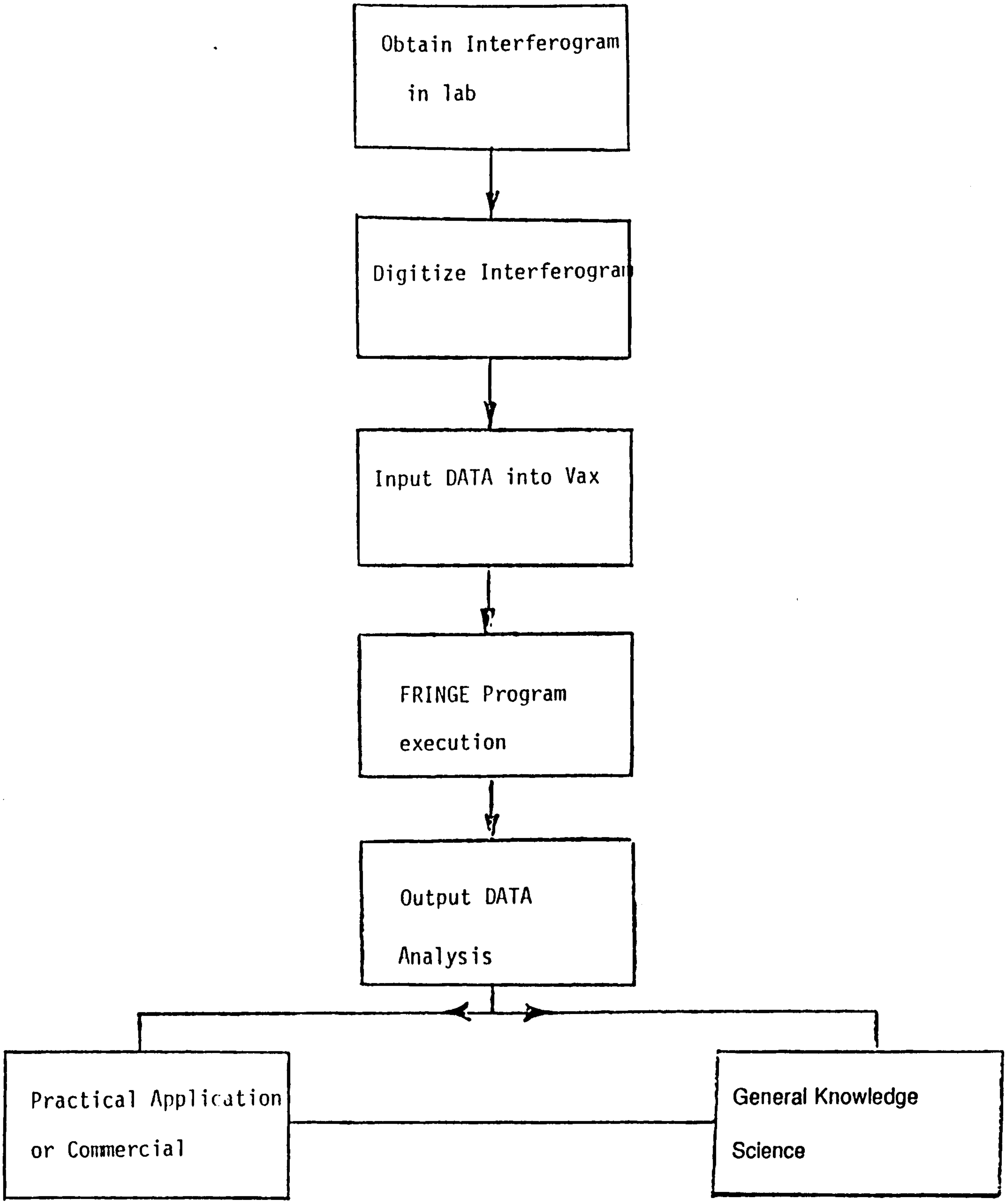

Figure E1.- Fringe analysis process flowchart.